Progress In Electromagnetics Research, Vol. 150, 123–143, 2015

Propagation of Partially Coherent Beam in Turbulent Atmosphere: A Review

Fei Wang, Xianlong Liu, and Yangjian Cai*

(*Invited Review*)

Abstract—Partially coherent beam is preferred in many applications, such as free-space optical communications, remote sensing, active laser radar systems, etc., due to its resistance to the deleterious effects of atmospheric turbulence. In this paper, after presenting a historical overview on propagation of optical beams in turbulent atmosphere, we describe the basic theory for treating the propagation of optical beams in turbulent atmosphere and we mainly introduce recent theoretical and experimental developments on propagation of partially coherent beam in turbulent atmosphere. Recent progress on the interaction of a partially coherent beam with a semirough target in turbulent atmosphere and the corresponding inverse problem are also reviewed.

1. INTRODUCTION

Recently, more and more attention is paid to the use of optical beams for free-space optical (FSO) communications due to the increasing requirement for larger bandwidths and high rate of data transfer in optical wavelength. The high direction of the optical beams can guarantee the security of the transmitted data to a certain extent in FSO communications compared to that in Radio-frequency (RF) communications. Furthermore, optical beams are also applied in other applications, such as laser satellite communications, laser radar system and remote sensing. In those applications, propagation of optical beam in atmosphere is inevitably encountered.

In general, there are three primary atmospheric phenomena, i.e., absorption, scattering and refractive-index fluctuation, affecting the propagation of optical beams through atmosphere. Absorption and scattering which cause energy attenuation of the optical beam upon propagation are caused by the constituent gas and particles in atmosphere. Refractive-index fluctuation which is commonly referred to as atmospheric turbulence is caused by the temperature differential between earth's surface and atmosphere. When a laser beam propagates through atmospheric turbulence, it experiences extra beam spreading, beam wander, scintillation (i.e., intensity fluctuation) and angle-of-arrival fluctuation. The presence of atmospheric turbulence greatly limits the performance of FSO communication, laser radar system and remote sensing, etc.. Therefore, it is of practical importance to study the propagation of laser beams in atmospheric turbulence and the methods to overcome or reduce the turbulence-induced degradation. Turbulence represents a nonlinear process which is governed by Navier-Stokes equations, while it is difficult to solve Navier-Stokes equations rigorously in mathematics. Thus, the turbulent theory commonly applied in the literature is based on a statistical method developed by Kolmogorov [1] and some additional simplifications and approximations, not derived from first principles.

The earliest theoretical study on the propagation of optical wave through turbulent media dated back to before the invention of laser beams. Tatarskii [2] and Chernov [3] published monographs on

Received 8 January 2015, Accepted 30 January 2015, Scheduled 6 February 2015

Invited paper for the Commemorative Collection on the 150-Year Anniversary of Maxwell's Equations.

* Corresponding author: Yangjian Cai (yangjiancai@suda.edu.cn).

The authors are with the College of Physics, Optoelectronics and Energy & Collaborative Innovation Center of Suzhou Nano Science and Technology, Soochow University, Suzhou 215006, China.

the propagation of optical plane waves and spherical waves through turbulence. Since then, various approaches including difference equations [4], transport methods [5], ladder approximation of the Bethe-Saltpeter equation [6] and the extended Huygens-Fresnel (eHF) principle [7] were introduced to investigate the propagation characteristics including coherence properties, average intensity and beam spreading, of optical beams propagation through turbulence. Among these approaches, eHF principle is widely used because it is somewhat easy to obtain analytical propagation formula. Yura obtained a general expression for the mutual coherence function (MCF) of a finite optical beam propagating in turbulent medium based on the eHF principle [8]. Feizulin and Kravtsov investigated the beam spreading of a laser beam propagating in turbulent medium with the help of the eHF method [9].

In 1972, Kon and Tatarskii considered the MCF of a partially coherent source in a turbulent medium and investigated the dependence of the average light intensity in turbulent medium on the initial degree of coherence of the source [10]. It seems to be the first publication to study the behavior of a partially coherent beam in turbulent atmosphere. In 1978, Leader derives expressions for the MCF and average intensity of a partially coherent beam in turbulent atmosphere based by using a Rayleigh-Sommerfeld integral method which is built on eHF principle [11]. Later, Wang and Plonus formulated the general expression for the mutual intensity function (i.e., MCF) of a partial coherent source in weakly turbulent atmosphere with the help of eHF principle and quadratic approximation [12].

Leader investigated the normalized intensity variance (a parameter to measure the strength of intensity fluctuation) of the optical beam which simulates laser reflectance from a rough surface with arbitrary height deviation in atmospheric turbulence [13]. Later, he extended his study to the intensity fluctuation of a partially coherent beam of arbitrary size and focus propagating through weak atmospheric turbulence [14]. In his study, the extended Rayleigh-Sommerfeld integral and the quadratic structure function (QSF) approximation for the fourth-order atmospheric spherical wave coherence function were applied. The effect of source temporal coherence on light scintillation in weak turbulence is studied by Fante [15]. Banach et al. explored the intensity fluctuation of a partially coherent beam in turbulent atmosphere and discussed two different cases: "fast" and "slow" detectors, which led to dramatic differences [16, 17]. Wang et al. studied the intensity fluctuation of a partially coherent beam propagating in atmosphere considering the aperture-effects in the receiver plane [18]. In those early studies, it was found that the scintillation of a partially coherent beam is smaller than a coherent beam in turbulent atmosphere, while no experimental results are reported, and the beam wander of a partially coherent beam propagating in atmosphere seems to be ignored. From 1990 to 2000, only few papers were devoted to the propagation of a partially coherent beam in atmospheric turbulence [19, 20].

With the advent of a variety of novel laser beams with prescribed beam profile, state of polarization and phase, several hundreds of papers were published on the propagation properties of novel laser beams in turbulent atmosphere since 2000. It was shown that a laser beam with prescribed beam profile, state of polarization, phase can reduce the turbulence-induced degradation. In the meantime, numerous papers were published on propagation of partially coherent beams with prescribe beam profile, state of polarization and phase, and it is interesting to find that such beams can further reduce turbulence-induced degradation, which will be quite useful in free-space optical communications, remote sensing and active laser radar systems.

In this paper, we outline the basic theory for treating the propagation of optical beam in turbulent atmosphere, and we mainly introduce recent theoretical and experimental developments on propagation of partially coherent beam in turbulent atmosphere. The interaction of a partially coherent beam with a semirough target in turbulent atmosphere and the corresponding inverse problem are also introduced.

2. SECOND-ORDER STATISTICAL PROPERTIES OF A PARTIALLY COHERENT BEAM IN TURBULENT ATMOSPHERE

The second-order statistical properties of a laser beam in turbulent atmosphere including average intensity, root mean squared (RMS) beam width, propagation factor and so on are closely related to the loss of the power and the effective receiver aperture size in the receiver, thus investigation of those properties is essential for practical applications. Cai and He investigated the average intensity of various flat-topped beams, dark hollow beams and elliptical Gaussian beam in turbulent atmosphere with the help of a tensor method [21–23]. Young et al. explored the average intensity and beam

spreading of high-order Gaussian beams including Hermite-Gaussian beams and Laguerre-Gaussian beams in atmospheric turbulence [24], and they found that high-order Gaussian beams experienced less percentage of additional broadening than the fundamental Gaussian beam due to turbulence. The propagation properties of non-diffractive beams such as Bessel-Gaussian beams and Airy beams in turbulent atmosphere were studied in [25, 26]. Furthermore, the propagation properties of laser beam arrays in turbulent atmosphere were reported in [27–30]. These studies came to the same results that the average intensity distributions of laser beams or beam arrays degenerated to Gaussian profiles at sufficient large propagation distance due to the isotropic effect of atmospheric turbulence, and those beams spread much faster in atmosphere than that in free space. Similar results were also found for other laser beams upon propagation in turbulent atmosphere [31–38]. The propagation of a laser beam through Target-in-the-loop (TIL) system in atmosphere was analyzed by Vorontsov and co-workers [39, 40].

In the meantime, the second-order statistical properties of a partially coherent beam in turbulent atmosphere also attract much attention in the past decade due to potential application in FSO communications. Beam spreading properties of a partially coherent beam in turbulent atmosphere was theoretically investigated by Gbur and Wolf [41], and it was revealed that partially coherent beams were less sensitive to turbulence. This interesting phenomenon was demonstrated in experiment by Dogariu and Amarande [42]. Shirai et al. studied the spreading of partially coherent beams propagating in atmospheric turbulence by use of the coherent-mode representation of the beams, and explained why partially coherent beams are less sensitive to turbulence from the aspect of mode decomposition [43]. Ricklin and Davidson revisited the effects of the atmospheric turbulence on propagation characteristics of a partially coherent beam and discussed its potential application in FSO communications [44, 45]. Since then, numerous efforts were devoted to study the second-order statistical properties of partially coherent beams in atmosphere. The model of partially coherent beam in the literature was not restricted to the well-known Gaussian-Schell model (GSM) beam. The behaviors of other types of partially coherent beams with prescribe beam profile and phase, such as partially coherent general beams [46], partially coherent higher-order Gaussian beams [47–53], partially coherent flat-topped beams [54, 55] and partially coherent dark hollow beams [56, 57], in turbulent atmosphere were also explored.

The statistical properties, especially the change of the polarization, of partially coherent vector beams upon propagation in turbulent atmosphere were also paid much attention in the past several years. Salem et al. analyzed the polarization changes of a partially coherent electromagnetic beam (i.e., partially coherent vector beam with spatially uniform state of polarization) in atmosphere [58]. Korotkova and co-workers investigated the change of the polarization ellipse and the far-field behaviors of the degree of polarization of a partially coherent electromagnetic beam propagating in atmospheric turbulence [59, 60]. It was found that the value of the degree of polarization recovered to its initial value in the source plane at sufficiently large propagation distance in turbulent atmosphere. The statistical properties of partially coherent electromagnetic beams under different conditions in turbulent atmosphere can be found in [61–67]. The statistical properties of a partially coherent vector beam with spatially non-uniform state of polarization can be found in [68, 69].

As mentioned in the introduction, the eHF principle was first introduced by Yura in 1972 and was used to evaluate the MCF of a Gaussian wave in turbulent medium [8]. In recent year, this principle was adopted by many researchers to explore the second-order statistical properties of light beams propagating in atmosphere. The numerical results obtained from eHF principle agreed reasonably well with the experimental results [70], even the phase approximation was used [71].

If $U(\mathbf{r}, 0)$ denotes the electric field of a light beam in the transmitter, the field of the light beam after propagating through turbulent medium with distance L is obtained through the eHF principle

$$U(\boldsymbol{\rho}, L) = -\frac{ik}{2\pi L} \int d^2\mathbf{r} U_0(\mathbf{r}, 0) \exp\left(\frac{ik\left(\boldsymbol{\rho} - \mathbf{r}\right)^2}{2L}\right) \exp\left(\psi(\mathbf{r}, \boldsymbol{\rho}, L)\right), \tag{1}$$

where $\mathbf{r}$ and $\boldsymbol{\rho}$ denote the position vectors in the transmitter plane and the receiver plane, respectively. $k = 2\pi/\lambda$ is the wave number with λ being the wavelength in vacuum. $\psi(\mathbf{r}, \boldsymbol{\rho}, L)$ is the random part of complex phase of a spherical wave propagating in turbulence for the point $(\mathbf{r}, 0)$ to the point $(\boldsymbol{\rho}, L)$. The schematic for the propagation geometry is shown in Figure 1. The angular frequency of the field is suppressed. Applying Eq. (11), the MCF (i.e., second-order correlation function) of a partially coherent

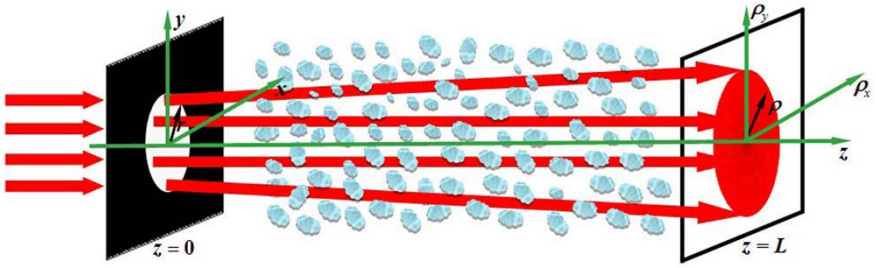

Figure 1. Schematic for the propagation of light beams in atmosphere.

beam in the receiver plane in turbulent atmosphere is obtained as

$$\Gamma(\boldsymbol{\rho}_1,\boldsymbol{\rho}_2,L)=\langle U(\boldsymbol{\rho}_1,L)U^*(\boldsymbol{\rho}_2,L)\rangle_s=-\frac{ik}{2\pi L}\int\Gamma_0(\mathbf{r}_1,\mathbf{r}_2,0)\exp\left[\frac{ik\left(\boldsymbol{\rho}_1-\mathbf{r}_1\right)^2}{2L}\right]$$
$$\times\exp\left[-\frac{ik\left(\boldsymbol{\rho}_2-\mathbf{r}_2\right)^2}{2L}\right]\langle\exp\left[\psi(\mathbf{r}_1,\boldsymbol{\rho}_1,L)+\psi^*(\mathbf{r}_2,\boldsymbol{\rho}_2,L)\right]\rangle_m d^2\mathbf{r}_1 d\mathbf{r}_2, \tag{2}$$

where $\Gamma_0(\mathbf{r}_1,\mathbf{r}_2,0)=\langle U_0(\mathbf{r}_1,0)U_0^*(\mathbf{r}_2,0)\rangle_s$ denotes the MCF of a partially coherent beam in the transmitter plane. The angular brackets denote the ensemble average. The subscript "s" and "m" represent the ensemble averages over the source fluctuation and the turbulent medium, respectively. We assume that the statistics between them is independent. The fourth-order correlation function of the partially coherent beam in the receiver plane in turbulent atmosphere is obtained as

$$\begin{aligned}\Gamma\left(\boldsymbol{\rho}_1,\boldsymbol{\rho}_2,\boldsymbol{\rho}_3,\boldsymbol{\rho}_4,L\right)&=\langle U\left(\boldsymbol{\rho}_1,L\right)U^*\left(\boldsymbol{\rho}_2,L\right)U(\boldsymbol{\rho}_3,L)U^*(\boldsymbol{\rho}_4,L)\rangle\\&=-\frac{ik}{2\pi L}\iiiint d^2\mathbf{r}_1d^2\mathbf{r}_2d^2\mathbf{r}_3d^2\mathbf{r}_4\left\langle U_0(\mathbf{r}_1,0)U_0^*\left(\mathbf{r}_2,0\right)U_0\left(\mathbf{r}_3,0\right)U_0^*\left(\mathbf{r}_4,0\right)\right\rangle_s\\&\quad\times\exp\left[\frac{ik\left(\boldsymbol{\rho}_1-\mathbf{r}_1\right)^2}{2L}-\frac{ik\left(\boldsymbol{\rho}_2-\mathbf{r}_2\right)^2}{2L}+\frac{ik\left(\boldsymbol{\rho}_3-\mathbf{r}_3\right)^2}{2L}-\frac{ik\left(\boldsymbol{\rho}_4-\mathbf{r}_4\right)^2}{2L}\right]\\&\quad\times\left\langle\exp\left[\psi(\mathbf{r}_1,\boldsymbol{\rho}_1,L)+\psi^*(\mathbf{r}_2,\boldsymbol{\rho}_2,L)+\psi(\mathbf{r}_3,\boldsymbol{\rho}_3,L)+\psi^*\left(\mathbf{r}_4,\boldsymbol{\rho}_4,L\right)\right]\right\rangle_m.\end{aligned} \tag{3}$$

According to [72, see in Chapter 7.3], the average term in Eq. (2) can be written as

$$\langle\exp\left[\psi(\mathbf{r}_1,\boldsymbol{\rho}_1,L)+\psi^*(\mathbf{r}_2,\boldsymbol{\rho}_2,L)\right]\rangle_m=\exp\left[2E_1(0,0,;0,0)+E_2(\boldsymbol{\rho}_1,\boldsymbol{\rho}_2;\mathbf{r}_1,\mathbf{r}_2)\right], \tag{4}$$

and the average term in Eq. (3) reads as

$$\begin{aligned}&\langle\exp\left[\psi(\mathbf{r}_1,\boldsymbol{\rho}_1,L)+\psi^*(\mathbf{r}_2,\boldsymbol{\rho}_2,L)+\psi(\mathbf{r}_3,\boldsymbol{\rho}_3,L)+\psi^*(\mathbf{r}_4,\boldsymbol{\rho}_4,L)\right]\rangle_m\\&=\exp\left[4E_1(0,0;0,0)+E_2(\boldsymbol{\rho}_1,\boldsymbol{\rho}_2;\mathbf{r}_1,\mathbf{r}_2)+E_2(\boldsymbol{\rho}_1,\boldsymbol{\rho}_4;\mathbf{r}_1,\mathbf{r}_4)+E_2(\boldsymbol{\rho}_3,\boldsymbol{\rho}_2;\mathbf{r}_3,\mathbf{r}_2)\right.\\&\quad\left.+E_2(\boldsymbol{\rho}_3,\boldsymbol{\rho}_4;\mathbf{r}_3,\mathbf{r}_4)+E_3(\boldsymbol{\rho}_1,\boldsymbol{\rho}_3;\mathbf{r}_1,\mathbf{r}_3)+E_3^*(\boldsymbol{\rho}_2,\boldsymbol{\rho}_4;\mathbf{r}_2,\mathbf{r}_4)\right].\end{aligned} \tag{5}$$

where E_1, E_2 and E_3 in Eqs. (4)–(5) are expressed as

$$E_1(0,0;0,0)=-2\pi^2k^2L\int_0^\infty\kappa\Phi_n(\kappa)d\kappa, \tag{6}$$

$$E_2(\boldsymbol{\rho}_1,\boldsymbol{\rho}_2;\mathbf{r}_1,\mathbf{r}_2)=4\pi^2k^2L\int_0^1\int_0^\infty\kappa\Phi_n(\kappa)J_0\left[\kappa\left|(1-\xi)\boldsymbol{\rho}_d+\xi\mathbf{r}_d\right|\right]d\xi d\kappa, \tag{7}$$

$$E_3(\boldsymbol{\rho}_1,\boldsymbol{\rho}_2;\mathbf{r}_1,\mathbf{r}_2)=-4\pi^2k^2L\int_0^1\int_0^\infty\kappa\Phi_n(\kappa)J_0\left[\kappa\left|(1-\xi)\boldsymbol{\rho}_d+\xi\mathbf{r}_d\right|\right]\times\exp\left[-\frac{iL\kappa^2}{k}\xi(1-\xi)\right]d\xi d\kappa, \tag{8}$$

where $\mathbf{r}_d=\mathbf{r}_1-\mathbf{r}_2$ and $\boldsymbol{\rho}_d=\boldsymbol{\rho}_1-\boldsymbol{\rho}_2$ are the difference of coordinates in the transmitter and in the receiver plane. $\Phi_n(\kappa)$ stands for the power spectral density of index-of-refraction fluctuation which reflects the statistical properties of the turbulent atmosphere.

To apply these formulae, we must know the model of the power spectral density. The well-know *Kolmogorov power-law spectrum* is defined as

$$\Phi_n(\kappa) = 0.033C_n^2\kappa^{-11/3}, \quad 1/L_0 \ll \kappa \ll 1/l_0, \tag{9}$$

where C_n^2 is the structure constant describing strength of the turbulence, L_0 and l_0 represent the outer scale and inner scale of turbulence, respectively. For the case of $C_n^2 < 10^{-13}\,\mathrm{m}^{-2/3}$, the turbulence is called "weak turbulence". For the case of $C_n^2 > 10^{-13}\,\mathrm{m}^{-2/3}$, the turbulence is called "strong turbulence". Due to its simple mathematical expression, the *Kolmogorov spectrum* is widely adopted for theoretical calculations in many literatures. However, the *Kolmogorov spectrum* is only valid under the condition of $1/L_0 \ll \kappa \ll 1/l_0$. In some calculations, the outer scale is assumed to be infinity and the inner scale is assumed to be quite small. In order to include the dissipation range $\kappa > 1/l_0$, the well-known power spectral density named Tatarskii spectrum is introduced and is expressed as follows

$$\Phi_n(\kappa) = 0.033C_n^2\kappa^{-11/3}\exp\left(-\kappa^2/\kappa_m^2\right), \quad \kappa \gg 1/L_0, \tag{10}$$

with $\kappa_m = 5.92/l_0$. The Tatarskii spectrum has a singularity at $\kappa = 0$ in the limiting case $1/L_0 \to 0$. The Kolmogorov spectrum and the Tatarskii spectrum are often modified in practice so that they are also finite and isotropic in the case $\kappa < 1/L_0$. One of such modified models is *von Karman spectrum*, given by

$$\Phi_n(\kappa) = 0.033C_n^2\frac{\exp\left(-\kappa^2/\kappa_m^2\right)}{\left(\kappa^2+\kappa_0^2\right)^{11/6}}, \quad 0 \le \kappa < \infty, \tag{11}$$

with $\kappa_0 = C_0/L_0$. Here C_0 is a scaling constant and its value is chosen depending on the practical application. Other modified models can be found in [72].

It is difficult to obtain analytical propagation formula for the MCF of light beam propagating through the turbulence. In order to obtain analytical expression, a quadratic approximation has been applied. Then the average term in Eq. (2) reduces to [12, 44]

$$\langle\exp\left[\psi\left(\mathbf{r}_1,\boldsymbol{\rho}_1,L\right)+\psi^*(\mathbf{r}_2,\boldsymbol{\rho}_2,L)\right]\rangle_m = \exp\left[-\frac{1}{\boldsymbol{\rho}_0^2}\left(\mathbf{r}_d^2+\mathbf{r}_d\cdot\boldsymbol{\rho}_d+\boldsymbol{\rho}_d^2\right)\right], \tag{12}$$

where $\boldsymbol{\rho}_0 = (0.546C_n^2k^2L)^{-3/5}$ is the coherence length of a spherical wave propagating in turbulence. On substituting Eq. (12) into Eq. (2), the analytical expression for the MCF of laser beams with different models can be obtained.

As an application example, we outline briefly the process for obtaining the analytical propagation formula for the MCF of a twisted anisotropic GSM beam (i.e., anisotropic GSM beam with twist phase) propagating in turbulent atmosphere by means of the eHF principle and the tensor method [73–75]. The MCF of the twist anisotropic GSM beam in the transmitter plane is expressed in the following tensor form [73, 74]

$$\Gamma_0(\tilde{\mathbf{r}},0) = \exp\left(-\frac{ik}{2}\tilde{\mathbf{r}}^T\mathbf{M}^{-1}\tilde{\mathbf{r}}\right), \tag{13}$$

where $\tilde{\mathbf{r}}^T = (\mathbf{r}_1,\mathbf{r}_2)$, "$T$" denotes the transpose of $\tilde{\mathbf{r}}$. $\mathbf{M}$ is a 4×4 partially coherent complex curvature tensor given by [73]

$$\mathbf{M}^{-1} = \begin{pmatrix} \mathbf{R}^{-1} - (i/2k)\left(\boldsymbol{\sigma}_I^2\right)^{-1} - (i/k)\left(\boldsymbol{\sigma}_g^2\right)^{-1} & (i/k)\left(\boldsymbol{\sigma}_g^2\right)^{-1} + \mu\mathbf{J} \\ (i/k)\left(\boldsymbol{\sigma}_g^2\right)^{-1} + \mu\mathbf{J} & \mathbf{R}^{-1} - (i/2k)\left(\boldsymbol{\sigma}_I^2\right)^{-1} - (i/k)\left(\boldsymbol{\sigma}_g^2\right)^{-1} \end{pmatrix}, \tag{14}$$

where $\boldsymbol{\sigma}_I^2$ and $\boldsymbol{\sigma}_g^2$ stand the transverse spot width matrix and the transverse coherence width matrix, respectively. $\mathbf{R}^{-1}$ is a wave-front curvature matrix. $\boldsymbol{\sigma}_I^2$, $\boldsymbol{\sigma}_g^2$ and $\mathbf{R}^{-1}$ are all 2×2 matrices with transpose symmetry given by:

$$\left(\boldsymbol{\sigma}_I^2\right)^{-1} = \begin{pmatrix} \sigma_{I11}^{-2} & \sigma_{I12}^{-2} \\ \sigma_{I21}^{-2} & \sigma_{I22}^{-2} \end{pmatrix}, \quad \left(\boldsymbol{\sigma}_g^2\right)^{-1} = \begin{pmatrix} \sigma_{g11}^{-2} & \sigma_{g12}^{-2} \\ \sigma_{g21}^{-2} & \sigma_{g22}^{-2} \end{pmatrix}, \quad \mathbf{R}^{-1} = \begin{pmatrix} R_{11}^{-1} & R_{12}^{-1} \\ R_{21}^{-1} & R_{22}^{-1} \end{pmatrix}. \tag{15}$$

J is an anti-symmetric matrix, given by

$$\mathbf{J} = \begin{pmatrix} 0 & 1 \\ -1 & 0 \end{pmatrix}. \tag{16}$$

μ is a scalar real-valued twist factor with the dimension of an inverse length, limited by the double inequality $0 \le \mu^2 \le [k^2 \det(\sigma_{g0}^2)]^{-1}$ due to the non-negativity requirement of Eq. (13). Eq. (13) can be considered as the general case of a Gaussian-Schell model beam which possesses astigmatism and twist phase. Eq. (12) can be expressed the following alternative tensor form

$$\langle \exp[\psi(\mathbf{r}_1, \boldsymbol{\rho}_1, z; \omega) + \psi^*(\mathbf{r}_2, \boldsymbol{\rho}_2, z; \omega)] \rangle_m = \exp\left[-\frac{ik}{2} \left(\tilde{\mathbf{r}}^T \tilde{\mathbf{P}} \tilde{\mathbf{r}} + \tilde{\mathbf{r}}^T \tilde{\mathbf{P}} \tilde{\boldsymbol{\rho}} + \tilde{\boldsymbol{\rho}}^T \tilde{\mathbf{P}} \tilde{\boldsymbol{\rho}} \right) \right], \tag{17}$$

with $\tilde{\mathbf{P}} = \frac{2}{ik\boldsymbol{\rho}_0^2} \begin{pmatrix} \mathbf{I} & -\mathbf{I} \\ -\mathbf{I} & \mathbf{I} \end{pmatrix}$. $\tilde{\boldsymbol{\rho}}^T = (\boldsymbol{\rho}_1, \boldsymbol{\rho}_2)$ with $\boldsymbol{\rho}_1$ and $\boldsymbol{\rho}_2$ being two arbitrary points in the receiver plane. Substituting Eqs. (13) and (17) into Eq. (2), after some arrangement, Eq. (2) can be expressed in the following tensor form

$$\begin{aligned} \Gamma(\tilde{\boldsymbol{\rho}}, L) = & \frac{1}{\lambda^2 \left[\det\left(\tilde{\mathbf{B}} \right) \right]^{1/2}} \int_{-\infty}^{\infty} \int_{-\infty}^{\infty} \Gamma_s(\tilde{\mathbf{r}}, 0) \exp\left[-\frac{ik}{2} \left(\tilde{\mathbf{r}}^T \tilde{\mathbf{B}}^{-1} \tilde{\mathbf{r}} - 2\tilde{\mathbf{r}}^T \tilde{\mathbf{B}}^{-1} \tilde{\boldsymbol{\rho}} + \tilde{\boldsymbol{\rho}}^T \tilde{\mathbf{B}}^{-1} \tilde{\boldsymbol{\rho}} \right) \right] \\ & \times \exp\left[-\frac{ik}{2} \left(\tilde{\mathbf{r}}^T \tilde{\mathbf{P}} \tilde{\mathbf{r}} + \tilde{\mathbf{r}}^T \tilde{\mathbf{P}} \tilde{\boldsymbol{\rho}} + \tilde{\boldsymbol{\rho}}^T \tilde{\mathbf{P}} \tilde{\boldsymbol{\rho}} \right) \right] d^2\mathbf{r}_1 d^2\mathbf{r}_2, \end{aligned} \tag{18}$$

where $\tilde{\mathbf{B}} = \begin{pmatrix} \mathbf{LI} & \mathbf{0} \\ \mathbf{0} & -\mathbf{LI} \end{pmatrix}$, $\tilde{\mathbf{P}} = \frac{2}{ik\boldsymbol{\rho}_0^2} \begin{pmatrix} \mathbf{I} & -\mathbf{I} \\ -\mathbf{I} & \mathbf{I} \end{pmatrix}$ with $\mathbf{I}$ is a 2×2 unit matrix. After some vector integration and tensor operation, we obtain the MCF of TAGSM beam in the receiver plane

$$\Gamma(\tilde{\boldsymbol{\rho}}, L) = \frac{1}{\left[\det\left(\tilde{\mathbf{B}} \mathbf{M}^{-1} + \tilde{\mathbf{I}} + \tilde{\mathbf{B}} \tilde{\mathbf{P}} \right) \right]^{1/2}} \exp\left[-\frac{ik}{2} \tilde{\boldsymbol{\rho}}^T \mathbf{M}_o \tilde{\boldsymbol{\rho}} \right], \tag{19}$$

where $\mathbf{M}_o = (\tilde{\mathbf{B}}^{-1} + \tilde{\mathbf{P}}) - (\tilde{\mathbf{B}}^{-1} - \tilde{\mathbf{P}}/2)(\mathbf{M}^{-1} + \tilde{\mathbf{B}}^{-1} + \tilde{\mathbf{P}})^{-1}(\tilde{\mathbf{B}}^{-1} - \tilde{\mathbf{P}}/2)$ is the partially coherent complex curvature tensor in the receiver plane and $\tilde{\mathbf{I}}$ denotes the 4×4 unit matrix. By setting $\boldsymbol{\rho} = \boldsymbol{\rho}_1 = \boldsymbol{\rho}_2$ in Eq. (19), the average intensity distribution in the received plane is obtained $\langle I(\boldsymbol{\rho}, L) \rangle = \Gamma(\tilde{\boldsymbol{\rho}}, L)$.

With the help of the tensor method, one can treat the propagation of a variety laser beams with prescribed beam profile, phase and polarization, such as partially coherent electromagnetic beam, flat-topped beam, dark hollow beam and Gaussian beam array, through turbulent atmosphere in an analytical way [21–23, 27, 65].

The property of the beam spreading of a partially coherent beam in atmospheric turbulence is characterized by the root-mean squared (RMS) width, defined by [9, 43]

$$\rho^2(z) = \frac{\iint \boldsymbol{\rho}^2 \langle I(\boldsymbol{\rho}, z) \rangle \, d^2\boldsymbol{\rho}}{\iint \langle I(\boldsymbol{\rho}, z) \rangle \, d^2\boldsymbol{\rho}}. \tag{20}$$

According to [37], Eq. (20) can be written a rather simple form, i.e.,

$$\rho^2(z) = \boldsymbol{\sigma}_I^2 + \boldsymbol{\sigma}_J^2 z^2 + F_2 z^3. \tag{21}$$

The first term of the right side in Eq. (21) represents the initial beam width of the partially coherent beam, and the second term denotes the beam spreading induced by the diffraction effect in free space propagation, proportional to the square of propagation distance z^2. The coefficient σ_J^2 is a measure of far-zone angular spread of beam in free space. The last term denotes the extra beam spreading due to the effect of turbulence, proportional to the triple power of the propagation distance z^3. The coefficient F_2 reads as

$$F_2 = \frac{2\pi^2}{3} \int_0^{\infty} \kappa^3 \Phi_n(\kappa) d\kappa. \tag{22}$$

F_2 in Eq. (22) only depends on the power density spectrum of the turbulence, irrespective of characteristics of the beam parameters. At sufficiently large propagation distance, the RMS beam width is mainly determined by the term $F_2 z^3$. That is the reason why the beam shape of an elliptical beam propagating through the atmospheric turbulence will become circular eventually. In fact, the beam shape of any other beam will become rotational symmetry in the far field because the RMS beam width of such beam is proportional to $F_2 z^3$.

Another useful method for obtaining the moments of the partially coherent beams in atmosphere is the Wigner distribution function (WDF), defined as [76, 77]

$$h(\boldsymbol{\rho}_s, \boldsymbol{\theta}, z) = \left(\frac{k}{2\pi}\right)^2 \int_{-\infty}^{\infty} \Gamma(\boldsymbol{\rho}_s, \boldsymbol{\rho}_d, z) \exp(-ik\boldsymbol{\theta} \cdot \boldsymbol{\rho}_d) d^2\boldsymbol{\rho}_d, \tag{23}$$

where $\boldsymbol{\rho}_s = (\boldsymbol{\rho}_1 + \boldsymbol{\rho}_2)/2$, $\Gamma(\boldsymbol{\rho}_s, \boldsymbol{\rho}_d; z)$ is the MCF in the receiver plane. $k\theta_x$ and $k\theta_y$ are the wave vector component along the x axis and y axis, respectively. The moments of the order $n_1 + n_2 + m_1 + m_2$ of the WDF for partially coherent beams in turbulence are given by

$$\left\langle \rho_x^{n_1} \rho_y^{n_2} \theta_x^{m_1} \theta_y^{m_2} \right\rangle = \frac{1}{P} \int_{-\infty}^{\infty} \rho_x^{n_1} \rho_y^{n_2} \theta_x^{m_1} \theta_y^{m_2} h(\boldsymbol{\rho}, \boldsymbol{\theta}, z) d^2\boldsymbol{\rho}_d d^2\boldsymbol{\theta} \tag{24}$$

with

$$P = \int_{-\infty}^{\infty} h(\boldsymbol{\rho}, \boldsymbol{\theta}, z) d^2\boldsymbol{\rho}_d d^2\boldsymbol{\theta} \tag{25}$$

P denotes the total power carried by the beams. In principle, Eq. (24) allows us to obtain arbitrary moments with the help of WDF. The WDF functions of partially coherent dark hollow beam, partially coherent flat-topped beam, twisted GSM beam and their related properties such as RMS beam width, effective radius of curvature and propagation factor can be found in [57, 78, 79].

3. SCINTILLATION OF A PARTIALLY COHERENT BEAM IN TURBULENT ATMOSPHERE

When a light beam propagates through atmosphere, it experiences the atmospheric turbulence caused by the random fluctuation of refractive index. The amplitude and phase of the light beam therefore are temporal variant due to the turbulence. The intensity fluctuation of an optical beam resulting from propagation through atmospheric turbulence is commonly referred to scintillation. Based on the Rytov method, the scintillation theory built in the early studies was applied in a variety of beams under the condition of weak turbulence [80–87]. The main motivation of this study was to find what kinds of light beams could reduce the scintillation index in the receiver plane. Fortunately, some laser beams posses such ability from the numerical simulation, and the experimental results for high-order beams have been reported to support such conclusions [88, 89].

Calculation of the scintillation of a partially coherent beam induced by the atmospheric turbulence seems to be more complicated compared to that of a coherent beam. In order to obtain analytical expression for the scintillation index, Feizulin and Kravtsov used the quadratic approximation in the two-source structure functions for a spherical wave propagating in a weakly turbulent atmosphere [9]. With the help of the quadratic approximation and eHF principle, the scintillation index of a partially coherent beam has been studied by Leader [13] and Wang et al. [18]. Recently, this method was applied to study the scintillation properties of other partially coherent beams with prescribed beam profile and phase [90, 91]. In 2004, Korotkova et al. [92] established an analytical model for evaluating the scintillation index of a GSM beam. In this model, a partially coherent beam is simulated by a laser beam passing through a random phase diffuser with Gaussian statistics, which is placed in the transmitter plane. Later, this model was applied for partially coherent electromagnetic beam [93]. Extension of this theoretical mode to other types of partially coherent beams has not been developed yet. Berman and Chumak [94] introduced photon distribution function to evaluate the scintillation index of a partially coherent beam for long-distance propagation. The equivalence of these methods has not been approved, but the results obtained from these methods are similar, e.g., the partially coherent beam can greatly reduce the scintillation induced by atmospheric turbulence.

The strength of the intensity fluctuation of the optical beam propagating through turbulence is measured by *scintillation index*, defined as

$$\sigma_I^2 = \frac{\left\langle I^2(\boldsymbol{\rho}; z)\right\rangle}{\left\langle I(\boldsymbol{\rho}; z)\right\rangle^2} - 1, \tag{26}$$

where $I(\boldsymbol{\rho};\, z)$ stands for the instantaneous intensity of an optical beam at point $\boldsymbol{\rho}$ in the receiver plane. The denominator is the square of the average intensity which can be evaluated from the second-order correlation function of the field shown in Eq. (2), and the numerator is the average of the square of the instantaneous intensity which can be derived from the fourth-order correlation function of the filed shown in Eq. (3).

To calculate the scintillation index, it is important for use to take the characteristic time of intensity fluctuation of the source τ_s, the response time of intensity fluctuation induced by the turbulence τ_a and the integration time of the detector τ_d into consideration. For the case of $\tau_d \gg \tau_s$, the detector only measures the average temporal intensity of the beam due to the source fluctuation, whereas for the case of $\tau_d \ll \tau_s$, the detector is sensitive to the intensity fluctuation of the source and those caused by the atmospheric turbulence. The term "fast detector" means that the response time of τ_d is faster than τ_s and τ_a, i.e., $\tau_d \ll \tau_s \ll \tau_a$. In this situation, the fourth-order moment of the field in the source plane is written

$$\left\langle U_0(\mathbf{r}_1,0)U_0^*(\mathbf{r}_2,0)U_0(\mathbf{r}_3,0)U_0^*(\mathbf{r}_4,0)\right\rangle_s = \Gamma_s\left(\mathbf{r}_1,\mathbf{r}_2\right)\Gamma_s(\mathbf{r}_3,\mathbf{r}_4) + \Gamma_s(\mathbf{r}_1,\mathbf{r}_4)\Gamma_s\left(\mathbf{r}_3,\mathbf{r}_2\right). \tag{27}$$

The term "slow detector" denotes the case $\tau_s \ll \tau_d \ll \tau_a$, and in this case, the fourth-order correlation function of the field in the source plane reduces

$$\left\langle U_0(\mathbf{r}_1,0)U_0^*(\mathbf{r}_2,0)U_0(\mathbf{r}_3,0)U_0^*(\mathbf{r}_4,0)\right\rangle_s = \Gamma_s(\mathbf{r}_1,\mathbf{r}_2)\Gamma_s(\mathbf{r}_3,\mathbf{r}_4). \tag{28}$$

Most of the literatures were devoted to investigate the scintillation index of a partially coherent beam under the condition of "slow detector". As an application example, we illustrate the process for evaluating the scintillation index of the twisted GSM in weak turbulence based on the eHF principle and the quadratic approximation for the average of the fourth-order phase term induced by the turbulence by applying the tensor method. According to Refs. [13, 18], the fourth-order spherical-wave coherence function of the turbulent medium is given by

$$\begin{aligned}
&\left\langle \exp\left[\psi^*\left(r_1,\boldsymbol{\rho}\right) + \psi\left(r_2,\boldsymbol{\rho}\right) + \psi^*\left(r_3,\boldsymbol{\rho}\right) + \psi\left(r_4,\boldsymbol{\rho}\right)\right]\right\rangle_m \\
&= \exp\left[-0.5D_\psi(r_1-r_2) - 0.5D_\psi(r_1-r_4) - 0.5D_\psi(r_2-r_3) - 0.5D_\psi(r_3-r_4)\right] \\
&\quad\times \exp\left[0.5D_\psi(r_2-r_4) + 0.5D_\psi(r_1-r_3)\right] \\
&\quad\times \exp\left[2B_x(r_2-r_4,0) + 2B_x(r_1-r_3)\right]\exp\left[iD_{xs}(r_2-r_4) - iD_{xs}(r_1-r_3)\right],
\end{aligned} \tag{29}$$

where $D_\psi(r_2-r_1) = 2|r_a-r_b|^2/\rho_0^2$, ($a$, b = 1, 2, 3, 4) is the wave structure function, $D_{xs}(r_a-r_b) = |r_a-r_b|^2/\rho_{xs}^2$ is the log-amplitude phase structure function with $\rho_{xs}^2 = (0.114k^{13/6}C_n^2z^{5/6})^{-1/2}$ is the coherence length of log-amplitude and phase. $B_x(r_a-r_b) = \sigma_{xs}^2 - 0.5(1/\rho_0^2 - 1/\rho_x^2)|r_a-r_b|$ is the log-amplitude correlation function, with $1/\rho_x^2 = 0.425C_n^2k^{13/6}z^{5/6}$ $\sigma_{xs}^2 = 0.124C_n^2k^{7/6}z^{11/6}$ is the variance of log amplitude for spherical wave.

Substituting Eq. (29) into Eq. (3), and after some arrangement, we can express the term $\langle I^2(\boldsymbol{\rho}, z)\rangle$in the following alternative tensor form:

$$\begin{aligned}
\left\langle I^2(\boldsymbol{\rho},z)\right\rangle = {}& \frac{\exp\left(4\sigma_{xs}^2\right)}{\lambda^4\det\left[\tilde{\mathbf{D}}\right]^{1/2}}\int_{-\infty}^{\infty}\int_{-\infty}^{\infty}\int_{-\infty}^{\infty}\int_{-\infty}^{\infty}\exp\left[-\frac{ik}{2}\tilde{\mathbf{r}}^T\tilde{\mathbf{N}}^{-1}\tilde{\mathbf{r}}\right]\exp\left[-\frac{ik}{2}\left(\tilde{\mathbf{r}}^T\tilde{\mathbf{D}}^{-1}\tilde{\mathbf{r}} - 2\tilde{\mathbf{r}}^T\tilde{\mathbf{D}}^{-1}\tilde{\boldsymbol{\rho}}\right)\right] \\
&\times\exp\left[-\frac{ik}{2}\tilde{\mathbf{r}}^T\tilde{\mathbf{Q}}\tilde{\mathbf{r}}\right]d^2\mathbf{r}_1d^2\mathbf{r}_2d^2\mathbf{r}_3d^2\mathbf{r}_4,
\end{aligned} \tag{30}$$

where $\tilde{\mathbf{r}}^T = (\mathbf{r}_1,\, \mathbf{r}_2,\, \mathbf{r}_3, \mathbf{r}_4)$ and $\tilde{\boldsymbol{\rho}}^T = (\boldsymbol{\rho},\, \boldsymbol{\rho},\, \boldsymbol{\rho},\, \boldsymbol{\rho})$ represent four arbitrary position vectors in the source plane and one position vector in the received plane. $\tilde{\mathbf{N}}$, $\tilde{\mathbf{D}}^{-1}$ and $\tilde{\mathbf{Q}}$ are 8×8 matrix given by:

$$\tilde{\mathbf{N}}^{-1} = \begin{pmatrix}\bar{\mathbf{M}}^{-1} & 0\\ 0 & \bar{\mathbf{M}}^{-1}\end{pmatrix},\quad \tilde{\mathbf{D}}^{-1} = \begin{pmatrix}\bar{\mathbf{B}}^{-1} & 0\\ 0 & \bar{\mathbf{B}}^{-1}\end{pmatrix},\quad \tilde{\mathbf{Q}} = \begin{pmatrix}\bar{\mathbf{Q}}_1 & \bar{\mathbf{Q}}_2\\ \bar{\mathbf{Q}}_2 & \bar{\mathbf{Q}}_1\end{pmatrix}, \tag{31}$$

with $\bar{\mathbf{Q}}_1$, $\bar{\mathbf{Q}}_2$ are given by

$$\begin{aligned}\bar{\mathbf{Q}}_1 &= \frac{2i}{k}\begin{pmatrix}\left(-2/\rho_0^2+1/\rho_x^2-i/\rho_{xs}^2\right)\bar{\mathbf{I}} & 1/\rho_0^2\bar{\mathbf{I}}\\ 1/\rho_0^2\bar{\mathbf{I}} & \left(-2/\rho_0^2+1/\rho_x^2+i/\rho_{xs}^2\right)\bar{\mathbf{I}}\end{pmatrix},\\ \bar{\mathbf{Q}}_2 &= \frac{2i}{k}\begin{pmatrix}-(1/\rho_x^2-i/\rho_{xs}^2)\bar{\mathbf{I}} & \left(1/\rho_0^2\right)\bar{\mathbf{I}}\\ 1/\rho_0^2\bar{\mathbf{I}} & -\left(1/\rho_x^2+i/\rho_{xs}^2\right)\bar{\mathbf{I}}\end{pmatrix}.\end{aligned} \tag{32}$$

After some rearrangement and vector integration, we obtain the expression for the intensity-correlation function

$$\left\langle I^2(\boldsymbol{\rho},z)\right\rangle = \exp\left(4\sigma_{xs}^2\right)\left[\det\left(\tilde{\mathbf{D}}\tilde{\mathbf{N}}^{-1}+\tilde{\mathbf{D}}\tilde{\mathbf{Q}}+\tilde{\mathbf{I}}\right)\right]^{-1/2}\exp\left[-\frac{ik}{2}\tilde{\boldsymbol{\rho}}^T\tilde{\mathbf{N}}_r^{-1}\tilde{\boldsymbol{\rho}}\right], \tag{33}$$

where $\tilde{\mathbf{N}}_r^{-1}=[(\tilde{\mathbf{N}}^{-1}+\tilde{\mathbf{Q}})^{-1}+\tilde{\mathbf{D}}]^{-1}$ and $\tilde{\mathbf{I}}$ is a 8×8 unit matrix. Substituting Eqs. (19) and (33) into Eq. (26), one can calculate the scintillation properties of the twisted GSM beam as well as the GSM beam propagating through weak turbulence [91]. It was found in [91] that the twist phase can greatly reduce the turbulence-induced scintillation.

Experimental study of the possibility for reduction of the scintillation index of a partially coherent beam with prescribed phase or polarization propagating through simulated atmosphere or real atmosphere has been carried out by several groups recently [95–99]. It was demonstrated that a partially coherent beam with initial radial polarization or vortex phase can further reduce the scintillation index. Here, we outline briefly our recent experimental development on the measurement of the scintillation index of the GSM vortex beam propagation through thermal-induced turbulence. The experimental setup for generating the GSM vortex beam, measuring its spatial coherence length and scintillation index is shown in Figure 2 [91].

Part I of Figure 2 is the experimental setup for generating a GSM vortex beam with controllable spatial coherence. A He-Ne laser beam ($\lambda\approx 632.8\,\mathrm{nm}$) reflected from a reflecting mirror focuses on the rotating ground-glass disk (RGGD) by a focal lens L_1, and then, passing through the collimating lens L_2 and the Gaussian amplitude filter (GAF), the beam becomes a GSM beam. GAF is used to transform its intensity into a Gaussian profile. After passing through a spiral phase plate (SPP) with transmission function $T(\varphi)=\exp(il\varphi)$ which is located just behind the GAF, the generated GSM beam becomes a GSMV beam, whose MCF is

$$\Gamma_{GSMV}(\mathbf{r}_1,\mathbf{r}_2)=\exp\left[-\frac{\mathbf{r}_1^2+\mathbf{r}_2^2}{4\sigma_0^2}-\frac{(\mathbf{r}_1-\mathbf{r}_2)^2}{2\sigma_g^2}\right]\exp\left[il(\varphi_1-\varphi_2)\right], \tag{34}$$

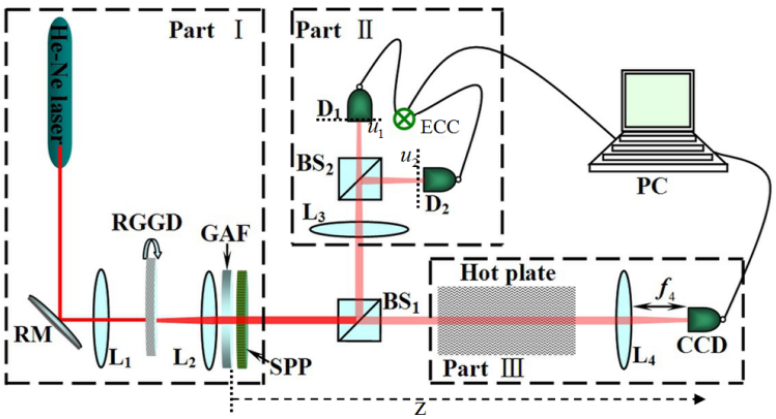

Figure 2. Experimental setup for generating a GSM vortex beam, measuring its spatial coherence length and the scintillation index of the generated beam propagating through thermally induced turbulence. RM, reflecting mirror; L_1, L_2, L_3, L_4, thin lenses; RGGD, rotating ground-glass disk; GAF, Gaussian amplitude filter; SPP, spiral phase plate; BS_1, BS_2, beam splitters; D_1, D_2, single photon detectors; ECC, electronic coincidence circuit; CCD, charge-coupled device; PC, personal computer.

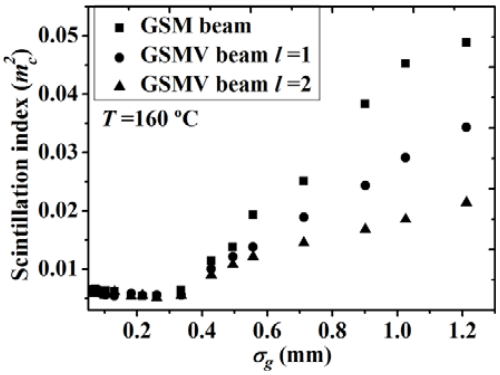

Figure 3. Experimental results of the scintillation index of a GSM or GSM vortex beam ($l = 1, 2$) at the centroid versus the initial coherence width.

where $\varphi_i = \arctan(y_i/x_i)$, l is the topological charge, and σ_0 and σ_g denote the transverse beam width and spatial coherence width, respectively.

Part II of Figure 2 shows the experimental setup for measuring the spatial coherence width σ_g of the generated GSM or GSM vortex beam. The detailed information of measuring process can be found in [96]. The transmitted beam from the BS_1 first passes through a 35 cm × 50 cm electric hot plate which is used to produce thermal turbulence through convection, then passes through a collection lens L_4 with focal length $f_4 = 15$ cm, and finally arrives at the charge-coupled device (CCD) locating in the geometrical focal plane (receiver plane), which is used to record the signal by a data acquisition system. Note that the intensity distribution of the GSM or GSM vortex beam in the plane of CCD is of Gaussian profile by controlling the spatial coherence length of the generated GSM vortex beam.

Figure 3 shows the experimental results of the scintillation index of a GSM vortex beam ($l = 1, 2$) at the centroid versus the initial spatial coherence width [98]. The corresponding results of a GSM beam are also shown in Figure 3. One finds from Figure 3 that the scintillation index of a GSM or GSMV beam decreases with the decrease of σ_g, indicating that a partially coherent beam with low value of σ_g is less affected by the turbulence as expected. When $\sigma_g > 0.35$ mm, the scintillation index of a GSM vortex beam is smaller than that of a GSM beam and the scintillation index decreases with the increase of the topological charge, which implies that a GSM vortex beam has advantage over a GSM beam for reducing turbulence-induced scintillation. When $\sigma_g < 0.35$ mm, the scintillation index of a GSM vortex beam is almost the same with that of a GSM beam, and almost doesn't vary as σ_g varies. This phenomenon could be explained by the fact that the scintillation index of the GSM vortex beam is influenced by the coherence and the vortex phase together, when σ_g is very small, the influence of the coherence on the scintillation index plays a dominant role, while the influence of the vortex phase is negligible.

Although many kinds of laser beams including partially coherent beams and high-order Gaussian beams have the potential to reduction of the scintillation index induced by the atmospheric turbulence, the RMS beam width is relative larger than the fundamental Gaussian beam under the same condition, which leads to the decrease of the intensity received by the detector in the receiver plane. Therefore, there is a trade-off between the beam spreading and the scintillation, and one should take both beam spreading and scintillation into consideration in a reasonable way in practical applications.

4. BEAM WANDER OF PARTIALLY COHERENT BEAM IN TURBULENT ATMOSPHERE

Besides the turbulence-induced beam spreading and scintillation, beam wander is another important factor caused by the turbulence which limits the performance of FSO communications, laser radar, and other areas. Upon propagation in atmospheric turbulence, a finite beam experiences random deflections. As a result, the beam spot observed at some distance from the transmitter will "dance" randomly in the transverse plane over short time periods, which is commonly referred to beam wander. Beam wander

can be characterized statistically by the variance of beam displacement along the propagation axis.

Up to now, many researchers have studied the effect of beam wander in atmospheric turbulence. Chernov [100] and Beckmann [101] used a geometrical optics method (GOM) to evaluate the wander of a single ray, not taking the diffraction effects and the finite beam size into consideration. Chiba derived an analytical formulation for the beam wander of a collimated or nearly collimated beam with finite beam size using GOM, and he carried out experiment for measuring the beam wander effect to compare his analytical results [102]. Churnside and Lataitis [103] developed the GOM and derived a simple, analytic expression for the variance of the beam displacement of light beam in atmosphere obeying the Kolmogorov statistics, which is applicable for the divergent or convergent Gaussian beam. Almost at the same time, an analysis of the beam wander that includes diffraction effects has also been developed by means on Markov approximation [104–106]. Tofsted analyzed the effect of the outer-scale of turbulence on the beam wander and the angle-of-arrival variance for the Gaussian beams [107].

Recently, the beam wanders of the high-order beams in turbulence have attracted more and more attentions. Eyyuboglu and Cil analyzed the beam wander of dark hollow (DH), flat-topped (FT) and annular beams in weak turbulence by means of Rytov approximation [108], and it was found that DH and FT beams exhibit less beam wander under certain conditions compared to the fundamental Gaussian beam. Similar results were found for cos, cosh-Gaussian beams and J_0-, I_0-Bessel Gaussian beams in the later papers [109, 110]. The influence of the vortex phase on the beam wander of laser beam in atmospheric turbulence was studied by Aksenov et al. using the Monte Carlo technique or the phase screen method [111, 112]. Wen and Chu investigated the beam wander of an Airy beam with a vortex phase in turbulence [113]. The results in those papers showed that the beam wander decreases as the topological charge of the vortex phase increases. Funes et al. carried out experimental measurement of the beam wander of a Gaussian beam against the propagation length through indoor artificially convective turbulence [114], and Kaushal et al. studied the beam wander of a Gaussian beam under varying atmospheric turbulence condition in an optical turbulence generator chamber [115].

In 2007, Berman et al. [116] used a photon distribution function method to examine the effect of initial spatial coherent length of a light beam on the beam wander in atmospheric turbulence, and they found that the beam wander decreases effectively with decrease of the initial spatial coherence length when the propagation distance is not very short. Xiao and Voelz [117] extended the beam wander theory of a focused coherent Gaussian beam in a weak turbulence developed by Andrews and Phillips [72, see in Chapter 6] to a focused partially coherent beam, and investigated the behavior of the beam wander of a focused partially coherent beam in atmosphere. Their theory is also applicable for the collimated or divergent partially coherent beam. Later, the influence of the polarization properties of the partially coherent electromagnetic beam on the beam wander was discussed by Song et al. [118]. Very recently, Liu et al. [119] verified in experiment that decreasing the spatial coherence length of the beam could indeed reduce the beam wander in the thermal-induced turbulence, and this advantage is enhanced when the spatial coherence length drops to a critical value which is determined by the propagation length and the beam characteristics.

Assume that the statistics of the atmospheric turbulence obey the Kolmogorov spectrum. Based on the Xiao's analysis [117], the variance of beam wander of the collimated partially coherent beam (GSM beam) takes the following form [119]

$$\left\langle r_c^2 \right\rangle = 7.25 C_n^2 \omega_0^{-1/3} L^3 \times \frac{48 - 33\left[1 + P\left(\sigma_g\right)\right]^{5/6} + 5\left[8P\left(\sigma_g\right) - 3\right]_2 F_1\left[1/6, 1/2, 3/2, -P\left(\sigma_g\right)\right]}{40P\left(\sigma_g\right)}, \quad (35)$$

with

$$P\left(\sigma_g\right) = \left(1 + \frac{\omega_0^2}{\sigma_g^2}\right)\frac{L^2}{z_R^2}, \quad (36)$$

where ω_0 and σ_g represent the beam waist size and the initial coherence length of the GSM beam, $z_R = k\omega_0^2/2$ denotes the Rayleigh length of the light beam, ${}_2F_1(\cdot)$ is a hypergeometric function. Eq. (35) is rather complicated and could not display the relationship between $\langle r_c^2 \rangle$ and σ_g clearly. In the limiting case $P(\sigma_g) \gg 1$ or $P(\sigma_g) \ll 1$, Eq. (35) can be simplified to the following analytical expression

$$\left\langle r_c^2 \right\rangle = \begin{cases} 12.39 C_n^2 \omega_0^{-1/3} z^3, & P\left(\sigma_g\right) \ll 1 \\ 3.88 k^{1/3} C_n^2 z^{8/3} \sigma_g^{1/3}, & P\left(\sigma_g\right) \gg 1 \end{cases} \quad (37)$$

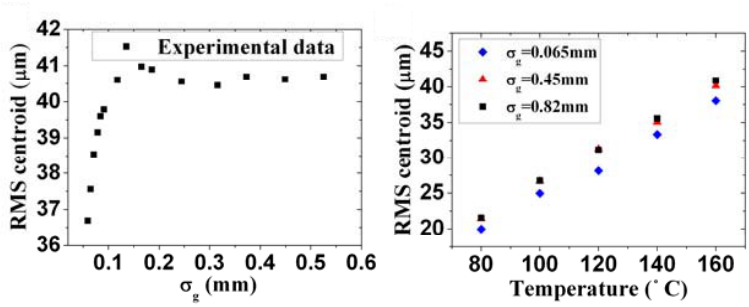

Figure 4. Experimental results of rms beam wander of the GSM beam versus (a) the transverse coherence length σ_g and (b) the temperature of the hot plate.

$P(\sigma_g) \gg 1$ means that the propagation distance is short, or the spatial coherence length is large compared to beam waist size, whereas $P(\sigma_g) \ll 1$ implies that the propagation distance is long or the spatial coherent length is smaller than the beam waist size. It follows from Eq. (37) that the variance of the beam wander is independent of spatial coherent length for the case $P(\sigma_g) \gg 1$, while the variance of beam wander decreases as the spatial coherent length decreases for the case $P(\sigma_g) \ll 1$.

Experimental verification of the dependence on the spatial coherent length on the RMS beam wander of the GSM beam is performed in Ref. [119]. The experimental setup is similar to Figure 2 (just remove the SPP in Figure 2). Figure 4 shows the experimental results of the RMS beam wander of the GSM beam against the spatial coherent length and the temperature of the hot plate through the thermal-induced turbulence. One finds that $\langle r_c^2 \rangle^{1/2}$ is almost independent of σ_g when the value of σ_g is about larger than 0.1 mm ($P(\sigma_g) \approx 0.25$), while $\langle r_c^2 \rangle^{1/2}$ decreases rapidly with the decrease of σ_g when the value of σ_g is smaller than 0.1 mm. As expected, $\langle r_c^2 \rangle^{1/2}$ increases with the increase of temperature, and the increasing slope is almost same for three different values of σ_g.

We want to point out that the reduction of the beam wander of the partially coherent beams sacrifices the beam divergence because the angular spread of the beam become far large with the decrease of the coherence length. Thus, it leads to the decrease of the intensity received by the detector in the receiver plane, and we should take those factors into consideration in practical applications.

5. INTERACTION OF A PARTIALLY COHERENT BEAM WITH A SEMIROUGH TARGET IN TURBULENT ATMOSPHERE

The interaction of a partially coherent beam with a semirough target in turbulent atmosphere has been studied in [120–122], and it was found that both the atmospheric turbulence and the target will induce changes of the spectral intensity, the degree of coherence, and the degree of polarization of the partially coherent beam. In [123], Sahin et al. analyzed the inverse problem of the interaction of a partially coherent electromagnetic beam with a semirough target in turbulent atmosphere, and they found that it is possible to predict the typical roughness of the target surface by comparing coherence and polarization properties of the illumination beam and of the return beam. In [124], with the help of the tensor method, Wu and Cai analyzed the inverse problem of the interaction of an isotropic GSM beam with a semirough target in turbulent atmosphere, and they found that we can determine the target size and the transverse correlation width of the target by measuring the transverse beam widths and the transverse coherence widths of the beams at the source plane and the receiver plane.

Figure 5 shows the schematic diagram for a GSM beam interacting with a semi-rough target in turbulent atmosphere and its equivalent (unfolded) version [124]. The MCF of an isotropic GSM beam without twist phase at the source plane is expressed in the following tensor form [124]

$$\Gamma(\tilde{\mathbf{r}}) = \exp\left(-\frac{ik}{2}\tilde{\mathbf{r}}^T \mathbf{M}_0^{-1} \tilde{\mathbf{r}}\right), \tag{38}$$

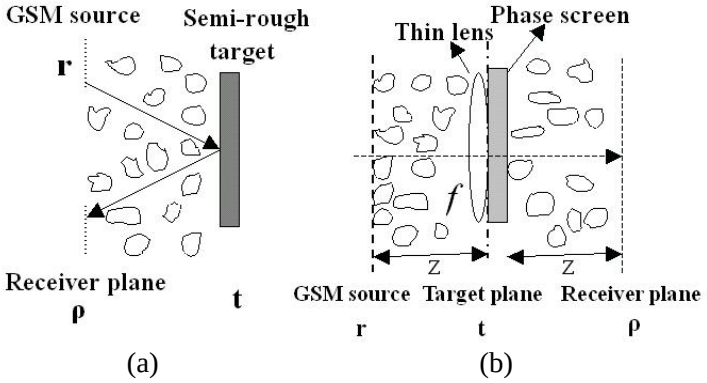

Figure 5. Schematic diagram for a GSM beam interacting with a semi-rough target in turbulent atmosphere and its equivalent (unfolded) version.

where $\mathbf{M}_0^{-1}$ is the complex curvature tensor given by

$$\mathbf{M}_0^{-1} = \begin{pmatrix} \left(-\dfrac{i}{2k\sigma_I^2} - \dfrac{i}{k\delta_I^2}\right)\mathbf{I} & \dfrac{i}{k\delta_I^2}\mathbf{I} \\ \dfrac{i}{k\delta_I^2}\mathbf{I} & \left(-\dfrac{i}{2k\sigma_I^2} - \dfrac{i}{k\delta_I^2}\right)\mathbf{I} \end{pmatrix}. \tag{39}$$

Here σ_s and δ_s denote the transverse beam width and the transverse coherence width of the GSM beam in the source plane. $\mathbf{I}$ is a 2×2 unit matrix.

The correlation function which describes the effect of the semirough target on the beam can be expressed in the following tensor form [124]

$$\langle T(\mathbf{t}_1)\, T^*(\mathbf{t}_2)\rangle = \frac{4\pi\beta^2}{k^2} \exp\left[-\frac{ik}{2}\tilde{\mathbf{t}}^T\tilde{\mathbf{T}}\tilde{\mathbf{t}}\right], \tag{40}$$

with

$$\tilde{\mathbf{T}} = \begin{pmatrix} \left(-\dfrac{2i}{k\omega_R^2} - \dfrac{2i}{kl_c^2}\right)\mathbf{I} & \dfrac{2i}{kl_c^2}\mathbf{I} \\ \dfrac{2i}{kl_c^2}\mathbf{I} & \left(-\dfrac{2i}{k\omega_R^2} - \dfrac{2i}{kl_c^2}\right)\mathbf{I} \end{pmatrix}. \tag{41}$$

Here ω_R denotes the target size, l_c the typical transverse correlation width which characterizes the roughness of the target, and β a normalization parameter.

After interaction with the target in atmospheric turbulence, we can obtain the MCF of the GSM beam in the receiver plane as follows [124]

$$\Gamma(\tilde{\boldsymbol{\rho}}) = \frac{4\pi\beta^2}{k^2\left[\det\left(\tilde{\mathbf{I}}+\tilde{\mathbf{B}}\mathbf{M}_1^{-1}+\tilde{\mathbf{B}}\tilde{\mathbf{T}}+\tilde{\mathbf{B}}\tilde{\mathbf{P}}_0\right)\right]^{1/2}\left[\det\left(\tilde{\mathbf{A}}+\tilde{\mathbf{B}}\mathbf{M}_0^{-1}+\tilde{\mathbf{B}}\tilde{\mathbf{P}}_0\right)\right]^{1/2}} \times \exp\left[-\frac{ik}{2}\tilde{\boldsymbol{\rho}}^T\mathbf{M}_2^{-1}\tilde{\boldsymbol{\rho}}\right]. \tag{42}$$

where $\tilde{\mathbf{I}}$ is a 4×4 unit matrix, $\mathbf{M}_2^{-1}$ is the complex curvature tensor of the GSM beam at the receiver plane given by

$$\mathbf{M}_2^{-1} = \tilde{\mathbf{P}}_0 + \tilde{\mathbf{B}}^{-1} - \left(\tilde{\mathbf{B}}^{-1} - 0.5\tilde{\mathbf{P}}_0\right)^T\left(\mathbf{M}_1^{-1} + \tilde{\mathbf{T}} + \tilde{\mathbf{B}}^{-1} + \tilde{\mathbf{P}}_0\right)^{-1}\left(\tilde{\mathbf{B}}^{-1} - 0.5\tilde{\mathbf{P}}_0\right). \tag{43}$$

Here

$$\tilde{\mathbf{A}} = \begin{pmatrix} \mathbf{I} & 0\mathbf{I} \\ 0\mathbf{I} & \mathbf{I} \end{pmatrix}, \quad \tilde{\mathbf{B}} = \begin{pmatrix} z\mathbf{I} & 0\mathbf{I} \\ 0\mathbf{I} & -z\mathbf{I} \end{pmatrix}, \quad \tilde{\mathbf{D}} = \begin{pmatrix} (1-z/f)\,\mathbf{I} & 0\mathbf{I} \\ 0\mathbf{I} & (1-z/f)\,\mathbf{I} \end{pmatrix}, \quad \tilde{\mathbf{P}} = \frac{2}{ik\rho_0^2}\begin{pmatrix} \mathbf{I} & -\mathbf{I} \\ -\mathbf{I} & \mathbf{I} \end{pmatrix}, \tag{44}$$

where $\rho_0 = (0.545C_n^2k^2z)^{-3/5}$ is the coherence length of a spherical wave propagating in the turbulent medium and C_n^2 the structure constant of the turbulent atmosphere.

We can express $\mathbf{M}_2^{-1}$ in the following alternative form

$$\mathbf{M}_2^{-1} = \begin{pmatrix} \left(R_{out}^{-1} - \dfrac{i}{2k\sigma_{out}^2} - \dfrac{i}{k\delta_{out}^2}\right)\mathbf{I} & \dfrac{i}{k\delta_{out}^2}\mathbf{I} \\ \dfrac{i}{k\delta_{out}^2}\mathbf{I} & \left(-R_{out}^{-1} - \dfrac{i}{2k\sigma_{out}^2} - \dfrac{i}{k\delta_{out}^2}\right)\mathbf{I} \end{pmatrix}, \tag{45}$$

where σ_{out} and δ_{out} are the transverse beam width and the transverse coherence width of the GSM beam at the receiver plane, and R_{out}^{-1} is its wave-front curvature.

After tedious operation, we can obtain the following equations

$$\frac{\rho_0^2}{\delta_{out}^2} = \frac{e_1\omega_R^4 + 4b_1\omega_R^2 + 2b_1 l_c^2 + f_1 l_c^2\omega_R^2 + g_1 l_c^2\omega_R^4}{a_1\omega_R^4 + 2b_1\omega_R^2 + b_1 l_c^2 + c_1 l_c^2\omega_R^2 + d_1 l_c^2\omega_R^4}, \tag{46}$$

$$\frac{1}{\sigma_{out}^2} = \frac{e_2 l_c^2\omega_R^2 + f_2 l_c^2\omega_R^4}{a_1\omega_R^4 + 2b_1\omega_R^2 + b_1 l_c^2 + c_1 l_c^2\omega_R^2 + d_1 l_c^2\omega_R^4}, \tag{47}$$

where

$$a_1 = 8R^2z^2\rho_0^2\delta^2\sigma^2, \quad b_1 = 16R^2z^2\rho_0^2\delta^2\sigma^4, \quad c_1 = R^2z^2\sigma^2\left[16\rho_0^2\sigma^2 + \delta^2\left(8\rho_0^2 + 32\sigma^2\right)\right],$$

$$d_1 = 8k^2Rz\rho_0^2\delta^2\sigma^4 + 4k^2z^2\delta^2\rho_0^2\sigma^4 + R^2\left[4k^2\rho_0^2\delta^2\sigma^4 + z^2\left(4\rho_0^2\sigma^2 + \delta^2\left(\rho_0^2 + 8\sigma^2\right)\right)\right],$$

$$e_1 = \rho_0^2R^2\delta^2\sigma^2\left(16z^2 + 8k^2\rho_0^2\sigma^2\right), \quad f_1 = R^2z^2\sigma^2\left[32\rho_0^2\sigma^2 + \delta^2\left(16\rho_0^2 + 48\sigma^2\right)\right],$$

$$g_1 = 24k^2Rz\rho_0^2\delta^2\sigma^4 + 8k^2z^2\rho_0^2\delta^2\sigma^4 + R^2\left[k^2\rho_0^2\left(24\delta^2 + 4\rho_0^2\right)\sigma^4 + z^2\left(8\rho_0^2\sigma^2 + \delta^2\left(2\rho_0^2 + 12\sigma^2\right)\right)\right],$$

$$e_2 = 16k^2R^2\rho_0^2\delta^2\sigma^4, \quad f_2 = 4k^2R^2\rho_0^2\delta^2\sigma^2, \quad \delta^2 = \frac{4k^2\rho_0^4\delta_I^2\sigma_I^4 + z^2\rho_0^2\left(4\rho_0^2\sigma_I^2 + \delta_I^2\left(\rho_0^2 + 8\sigma_I^2\right)\right)}{k^2\rho_0^2\left(24\delta_I^2 + 4\rho_0^2\right)\sigma_I^4 + z^2\left(8\rho_0^2\sigma_I^2 + \delta_I^2\left(2\rho_0^2 + 12\sigma_I^2\right)\right)},$$

$$\sigma^2 = \frac{4k^2\rho_0^2\delta_I^2\sigma_I^4 + z^2\left(4\rho_0^2\sigma_I^2 + \delta_I^2\left(\rho_0^2 + 8\sigma_I^2\right)\right)}{4k^2\rho_0^2\delta_I^2\sigma_I^2}, \quad \frac{1}{R} = -\frac{1}{f} + \frac{z\left(\rho_0^2\sigma_0^2 + \delta_0^2\left(0.25\rho_0^2 + 3\sigma_0^2\right)\right)}{k^2\rho_0^2\delta_0^2\sigma_0^4 + z^2\left(\rho_0^2\sigma_0^2 + \delta_0^2\left(0.25\rho_0^2 + 2\sigma_0^2\right)\right)}.$$

Through solving Eqs. (46) and (47), one can obtain the relations between ω_R, l_c, σ_s, δ_s, σ_{out}, δ_{out}, and one can determine the values of ω_R, l_c through measuring the values of σ_s, δ_s, σ_{out}, δ_{out} [124]. The values of beam widths σ_s and σ_{out} can be measured by the CCD conveniently, and the values of the coherence widths δ_s and δ_{out} can be measured by the method developed in [125]. Thus, GSM beam provides a convenient way for remote detection.

6. CONCLUSION

We have presented a historical overview on propagation of optical beams in turbulent atmospheric and introduced the basic theory for treating the propagation of optical beams in turbulent atmosphere. Recent progress on propagation of partially coherent beam in turbulent atmosphere, the interaction of partially coherent beam with a semirough target and corresponding inverse problem, has been reviewed. It was shown that the use of partially coherent beam may overcome the turbulence-induced beam degeneration, reduce the turbulence-induced scintillation, reduce the turbulence-induced beam wander, thus it has great potential application in FSO communications and active laser radar systems. Furthermore, partially coherent beam provides a convenient way for detecting a semirough target in turbulent atmosphere. Recently, experimental generation and measurement of a partially coherent beam with prescribed beam profile, polarization, phase and correlation function have been developed rapidly [126–140], and we believe that partially coherent beams will be used in many practical applications soon. A recent review on partially coherent beam propagation in atmospheric turbulence can be found in [141], which presents the progress in this field from another aspect.

ACKNOWLEDGMENT

This work is supported by the National Natural Science Foundation of China under Grant Nos. 11474213 & 11274005, the Project Funded by the Priority Academic Program Development of Jiangsu Higher Education Institutions, the Innovation Plan for Graduate Students in the Universities of Jiangsu Province under Grant No. KYZZ_0334, and the Project Sponsored by the Scientific Research Foundation for the Returned Overseas Chinese Scholars, State Education Ministry.

REFERENCES

1. Kolmogorov, A. N., "The local structure of turbulence in incompressible viscous fluid for very large Reynolds numbers," *Doklady Akademiia Nauk SSSR*, Vol. 30, No. 4, 301–305, 1941.
2. Tatarskii, V. I., *Wave Propagation in a Turbulent Medium,* McGraw-Hill, 1961.
3. Chernov, L. A., *Wave Propagation in a Random Medium,* McGraw-Hill, 1960.
4. Beran, M. J., "Propagations of a finite beam in a random medium," *J. Opt. Soc. Am.*, Vol. 60, No. 4, 518–521, 1970.
5. Fante, R. L., "Mutual coherence function and frequency spectrum of a laser beam propagating through atmospheric turbulence," *J. Opt. Soc. Am.*, Vol. 64, No. 5, 592–598, 1974.
6. Brown, W. P., "Second moment of a wave propagating in a random medium," *J. Opt. Soc. Am.*, Vol. 61, No. 8, 1051–1059, 1971.
7. Lutomirski, R. F. and H. T. Yura, "Propagation of a finite optical beam in an inhomogeneous medium," *Appl. Opt.*, Vol. 10, No. 7, 1652–1658, 1971.
8. Yura, H. T., "Mutual coherence function of a finite cross section optical beam propagating in a turbulent medium," *Appl. Opt.*, Vol. 11, No. 6, 1399–1406, 1972.
9. Feizulin, Z. I. and Y. A. Kravtsov, "Broadening of a laser beam in a turbulent medium," *Radiophys. Quantum Electron.*, Vol. 10, No. 1, 33–35, 1967.
10. Kon, A. I. and V. I. Tatarskii, "On the theory of the propagation of partially coherent light beams in a turbulent atmosphere," *Radiophys. Quantum Electron.*, Vol. 15, No. 10, 1187–1192, 1972.
11. Leader, J. C., "Atmospheric propagation of partially coherent radiation," *J. Opt. Soc. Am.*, Vol. 68, No. 2, 175–185, 1978.
12. Wang, S. C. H. and M. A. Plonus, "Optical beam propagation for a partially coherent source in the turbulent atmosphere," *J. Opt. Soc. Am.*, Vol. 69, No. 9, 1297–1304, 1979.
13. Leader, J. C., "Intensity fluctuations resulting from partially coherent light propagating through atmospheric turbulence," *J. Opt. Soc. Am.*, Vol. 69, No. 1, 73–84, 1979.
14. Leader, J. C., "Beam-intensity fluctuations in atmospheric turbulence," *J. Opt. Soc. Am.*, Vol. 71, No. 5, 542–558, 1981.
15. Fante, R. L., "The effect of source temporal coherence on light scintillations in weak turbulence," *J. Opt. Soc. Am.*, Vol. 69, No. 1, 71–73, 1979.
16. Banach, V. A., V. M. Buldakov, and V. L. Mironov, "Intensity fluctuations of the partially coherent light-beam in a turbulent atmosphere," *Opt. Spectrosc.*, Vol. 54, No. 6, 1054–1059, 1983.
17. Banakh, V. A. and V. M. Buldakov, "Effect of the initial degree of light-beam spatial coherence on intensity fluctuations in turbulent atmospheres," *Opt. Spectrosc.*, Vol. 55, No. 4, 707–712, 1983.
18. Wang, S. J., Y. Baykal, and M. A. Plonus, "Receiver-aperture averaging effects for the intensity fluctuation of a beam wave in the turbulent atmosphere," *J. Opt. Soc. Am.*, Vol. 73, No. 6, 831–837, 1983.
19. Wu, J., "Propagation of a Gaussian-Schell beam through turbulent media," *J. Mod. Opt.*, Vol. 37, No. 4, 671–684, 1990.
20. Wu, J. and A. D. Boardman, "Coherence length of a Gaussian-Schell beam and atmospheric turbulence," *J. Mod. Opt.*, Vol. 38, No. 7, 1355–1363, 1991.
21. Cai, Y. and S. He, "Propagation of various dark hollow beams in a turbulent atmosphere," *Opt. Express*, Vol. 14, No. 4, 1353–1367, 2006.

22. Cai, Y., "Propagation of various flat-topped beams in a turbulent atmosphere," *J. Opt. A*, Vol. 8, No. 6, 537–545, 2006.
23. Cai, Y. and S. He, "Average intensity and spreading of an elliptical Gaussian beam propagating in a turbulent atmosphere," *Opt. Lett.*, Vol. 31, No. 5, 568–570, 2006.
24. Young, C. Y., Y. V. Gilchrest, and B. R. Macon, "Turbulence induced beam spreading of higher order mode optical waves," *Opt. Eng.*, Vol. 41, No. 5, 1097–1103, 2002.
25. Eyyuboglu, H. T., "Propagation of higher order Bessel-Gaussian beams in turbulence," *Appl. Phys. B*, Vol. 88, No. 2, 259–265, 2007.
26. Chu, X., "Evolution of an Airy beam in turbulence," *Opt. Lett.*, Vol. 36, No. 14, 2701–2703, 2011.
27. Cai, Y., Y. Chen, H. T. Eyyuboglu, and Y. Baykal, "Propagation of laser array beams in a turbulent atmosphere," *Appl. Phys. B*, Vol. 88, No. 3, 467–475, 2007.
28. Zhou, P., X. Wang, Y. Ma, H. Ma, X. Xu, and Z. Liu, "Propagation property of a nonuniformly polarized beam array in turbulent atmosphere," *Appl. Opt.*, Vol. 50, No. 9, 1234–1239, 2011.
29. Chen, C., H. Yang, M. Kavehrad, and Z. Zhou, "Propagation of radial Airy array beams through atmospheric turbulence," *Optics and Lasers in Engineering*, Vol. 52, 106–114, 2014.
30. Ji, X. and Z. Pu, "Effective Rayleigh range of Gaussian array beams propagating through atmospheric turbulence," *Opt. Commun.*, Vol. 283, No. 20, 3884–3890, 2010.
31. Yuan, Y., Y. Cai, Q. Jun, H. T. Eyyuboglu, and Y. Baykal, "Average intensity and spreading of an elegant Hermite-Gaussian beam in turbulent atmosphere," *Opt. Express*, Vol. 17, No. 13, 11130–11139, 2009.
32. Eyyuboglu, H. T. and Y. Baykal, "Average intensity and spreading of cosh-Gaussian beams in turbulent atmosphere," *Appl. Opt.*, Vol. 44, No. 6, 976–983, 2005.
33. Qu, J., Y. Zhong, Z. Cui, and Y. Cai, "Elegant Laguerre-Gaussian beam in a turbulent atmosphere," *Opt. Commun.*, Vol. 283, No. 14, 2772–2781, 2010.
34. Zhou, P., X. Wang, Y. Ma, H. Ma, X. Xu, and Z. Liu, "Average intensity and spreading of a Lorentz beam propagating in a turbulent atmosphere," *J. Opt.*, Vol. 12, No. 1, 015409, 2010.
35. Wang, T., J. Pu, and Z. Chen, "Beam spreading and topological charge of vortex beams propagating in a turbulent atmosphere," *Opt. Commun.*, Vol. 282, No. 7, 1255–1259, 2009.
36. Ji, X. and X. Li, "Propagation properties of apertured laser beams with amplitude modulations and phase fluctuations through atmospheric turbulence," *Appl. Phys. B*, Vol. 104, No. 1, 207–213, 2011.
37. Aksenov, V. P., F. Y. Kanev, and C. E. Pogutsa, "Spatial coherence, mean wave tilt, and mean local wave-propagation vector of a Laguerre-Gaussian beam passing through a random phase screen," *Atmospheric and Oceanic Optics*, Vol. 23, No. 5, 344–352, 2010.
38. Valerii, A. P. and C. E. Pogutsa, "Optical Scully vortex and its spatial evolution," *Appl. Opt.*, Vol. 51, No. 10, 140–143, 2012.
39. Vorontsov, M. and V. Kolosov, "Target-in-the-loop beam control: Basic considerations for analysis and wave-front sensing," *J. Opt. Soc. Am.*, Vol. 22, No. 1, 126–141, 2005.
40. Mikhail, V. A., V. Kolosov, and E. Polnau, "Target-in-the-loop wavefront sensing and control with a Collett-Wolf beacon: Speckle-average phase conjugation," *Appl. Opt.*, Vol. 48, No. 1, 13–29, 2009.
41. Gbur, G. and E. Wolf, "Spreading of partially coherent beams in random media," *J. Opt. Soc. Am. A*, Vol. 19, No. 8, 1592–1598, 2002.
42. Dogariu, A. and S. Amarande, "Propagation of partially coherent beams: Turbulence-induced degradation," *Opt. Lett.*, Vol. 28, No. 1, 10–12, 2003.
43. Shirai, T., A. Dogariu, and E. Wolf, "Mode analysis of spreading of partially coherent beams propagating through atmospheric turbulence," *J. Opt. Soc. Am. A*, Vol. 20, No. 6, 1094–1102, 2003.
44. Ricklin, J. C. and F. M. Davidson, "Atmospheric turbulence effects on a partially coherent Gaussian beam: Implications for free-space laser communication," *J. Opt. Soc. Am. A*, Vol. 19, No. 9, 1794–1802, 2002.

45. Ricklin, J. C. and F. M. Davidson, "Atmospheric optical communication with a Gaussian-Schell beams," *J. Opt. Soc. Am. A*, Vol. 20, No. 5, 856–866, 2003.
46. Eyyuboglu, H. T., Y. Baykal, and Y. Cai, "Complex degree of coherence for partially coherent general beams in atmospheric turbulence," *J. Opt. Soc. Am. A*, Vol. 24, No. 9, 2891–2901, 2007.
47. Wang, D., F. Wang, Y. Cai, and J. Chen, "Evolution properties of the complex degree of coherence of a partially coherent Laguerre-Gaussian beam in turbulent atmosphere," *J. Mod. Opt.*, Vol. 59, No. 4, 372–380, 2012.
48. Ji, X. and X. Li, "Effective radius of curvature of partially coherent Hermite-Gaussian beams propagating through atmospheric turbulence," *J. Opt.*, Vol. 12, No. 3, 035403, 2010.
49. Wang, F., Y. Cai, H. T. Eyyuboglu, and Y. Baykal, "Average intensity and spreading of partially coherent standard and elegant Laguerre-Gaussian beams in turbulent atmosphere," *Progress In Electromagnetics Research*, Vol. 103, 33–56, 2010.
50. Aksenov, V. P., F. Y. Kanev, and C. E. Pogutsa, "Mean energy distribution and averaged pattern of optical vortices of a partially coherent light beam propagating in a randomly inhomogeneous atmosphere," *Proc. SPIE*, Vol. 7388, 738807, 2009.
51. Yang, A., E. Zhang, X. Ji, and B. Lu, "Angular spread of partially coherent Hermite-cosh-Gaussian beams propagating through atmospheric turbulence," *Opt. Express*, Vol. 16, No. 12, 8366–8380, 2008.
52. Li, J., A. Yang, and B. Lu, "Comparative study of the beam-width spreading of partially coherent Hermite-sinh-Gaussian beams in atmospheric turbulence," *J. Opt. Soc. Am. A*, Vol. 25, No. 11, 2670–2679, 2008.
53. Wang, F., Y. Cai, H. T. Eyyuboglu, and Y. Baykal, "Partially coherent elegant Hermite-Gaussian beam in turbulent atmosphere," *Appl. Phys. B*, Vol. 103, No. 2, 461–469, 2011.
54. Alavinejad, M., M. Khatiri, and B. Ghafary, "Transmittance of partially coherent flat topped beam with circular and elliptical symmetry in turbulence," *Opt. Commun.*, Vol. 282, No. 17, 3541–3546, 2009.
55. Alavinejad, M. and B. Ghafary, "Turbulence-induced degradation properties of partially coherent flat-topped beams," *Optics and Lasers in Engineering*, Vol. 46, No. 5, 357–362, 2008.
56. Wang, H. and X. Li, "Propagation of partially coherent controllable dark hollow beams with various symmetries in turbulent atmosphere," *Optics and Lasers in Engineering*, Vol. 48, No. 1, 48–57, 2010.
57. Yuan, Y., Y. Cai, J. Qu, H. T. Eyyuboglu, Y. Baykal, and O. Korotkova, "M_2-factor of coherent and partially coherent dark hollow beams propagating in turbulent atmosphere," *Opt. Express*, Vol. 17, No. 20, 17344–17356, 2009.
58. Salem, M., O. Korotkova, A. Dogariu, and E. Wolf, "Polarization changes in partially coherent electromagnetic beams propagating through turbulent atmosphere," *Waves in Random Media*, Vol. 14, No. 4, 513–523, 2004.
59. Korotkova, O., M. Salem, A. Dogariu, and E. Wolf, "Changes in polarization ellipse of random electromagnetic beams propagating through the turbulent atmosphere," *Waves in Random and Complex Media*, Vol. 15, No. 3, 353–364, 2005.
60. Korotkova, O., M. Salem, and E. Wolf, "The far-zone behavior of the degree of polarization electromagnetic beams propagating through atmospheric turbulence," *Opt. Commun.*, Vol. 233, Nos. 4–6, 225–230, 2004.
61. Du, X., D. Zhao, and O. Korotkova, "Changes in the statistical properties of stochastic anisotropic electromagnetic beams on propagation in the turbulent atmosphere," *Opt. Express*, Vol. 15, No. 25, 16909–16915, 2007.
62. Wu, G., B. Luo, S. Yu, A. Dang, and H. Guo, "The propagation of electromagnetic Gaussian-Schell model beams through atmospheric turbulence in a slanted path," *J. Opt.*, Vol. 13, No. 3, 035706, 2011.
63. Lu, W., L. Liu, J. Sun, Q. Yang, and Y. Zhu, "Change in degree of coherence of partially coherent electromagnetic beams propagating through atmospheric turbulence," *Opt. Commun.*, Vol. 271,

No. 1, 1–8, 2007.

64. Zhu, Y. and D. Zhao, "Propagation of a stochastic electromagnetic Gaussian Schell-model beam through an optical system in turbulent atmosphere," *Appl. Phys. B*, Vol. 96, No. 1, 155–160, 2009.
65. Cai, Y., O. Korotkova, H. T. Eyyuboglu, and Y. Baykal, "Active laser radar systems with stochastic electromagnetic beams in turbulent atmosphere," *Opt. Express*, Vol. 16, No. 20, 15834–15846, 2008.
66. Roychowdhury, H., S. A. Ponomarenko, and E. Wolf, "Change in the polarization of partially coherent electromagnetic beams propagating through the turbulent atmosphere," *J. Mod. Opt.*, Vol. 52, No. 11, 1611–1618, 2005.
67. Chen, Z. and J. Pu, "Propagation characteristics of aberrant stochastic electromagnetic beams in a turbulent atmosphere," *J. Opt. A*, Vol. 9, No. 12, 1123–1130, 2007.
68. Wang, H., D. Liu, and Z. Zhou, "The propagation of radially polarized partially coherent beam through an optical system in turbulent atmosphere," *Appl. Phys. B*, Vol. 101, Nos. 1–2, 361–369, 2010.
69. Chen, R., Y. Dong, F. Wang, and Y. Cai, "Statistical properties of a cylindrical vector partially coherent beam in turbulent atmosphere," *Appl. Phys. B*, Vol. 112, No. 2, 247–259, 2013.
70. Banakh, V. A., G. M. Krekov, V. L. Mironov, S. S. Khmelevtsov, and R. S. Tsvik, "Focused-laser-beam scintillations in the turbulent atmosphere," *J. Opt. Soc. Am.*, Vol. 64, No. 4, 516–518, 1974.
71. Banakh, V. A. and V. L. Mironov, "Phase approximation of the Huygens-Kirchhoff method in problems of laser-beam propagation in the turbulent atmosphere," *Opt. Lett.*, Vol. 1, No. 5, 172–174, 1977.
72. Andrews, L. C. and R. L. Phillips, *Laser Beam Propagation through Random Media,* SPIE, 1998.
73. Lin, Q. and Y. Cai, "Tensor ABCD law for partially coherent twisted anisotropic Gaussian-Schell model beams," *Opt. Lett.*, Vol. 27, No. 4, 216–218, 2002.
74. Cai, Y. and S. He, "Propagation of a partially coherent twisted anisotropic Gaussian Schell-model beam in a turbulent atmosphere," *Appl. Phys. Lett.*, Vol. 89, No. 4, 041117, 2006.
75. Simon, R., E. C. G. Sudarshan, and N. Mukunda, "Anisotropic Gaussian Schell-model beams: Passage through optical systems and associated invariants," *Phys. Rev. A*, Vol. 31, No. 4, 2419–2434, 1985.
76. Serna, J., R. Martinez-Herrero, and P. M. Mejias, "Parametric characterization of general partially coherent beams propagating through ABCD optical system," *J. Opt. Soc. Am. A*, Vol. 8, No. 7, 1094–1098, 1991.
77. Dan, Y. and B. Zhang, "Second moments of partially coherent beams in atmospheric turbulence," *Opt. Lett.*, Vol. 34, No. 5, 563–565, 2009.
78. Wang, F. and Y. Cai, "Second-order statistics of a twisted Gaussian Schell-model beam in turbulent atmosphere," *Opt. Express*, Vol. 18, No. 24, 24661–24672, 2010.
79. Dan, Y. and B. Zhang, "Beam propagation factor of partially coherent flat-topped beams in a turbulent atmosphere," *Opt. Express*, Vol. 16, No. 20, 15563–15575, 2008.
80. Baykal, Y. and H. T. Eyyuboglu, "Scintillation index of flat-topped Gaussian beams," *Appl. Opt.*, Vol. 45, No. 16, 3793–3797, 2006.
81. Peleg, A. and J. V. Moloney, "Scintillation index for two Gaussian laser beams with different wavelengths in weak atmospheric turbulence," *J. Opt. Soc. Am. A*, Vol. 23, No. 12, 3114–3122, 2006.
82. Eyyuboglu, H. T. and Y. Baykal, "Scintillations of cos-Gaussian and annular beams," *J. Opt. Soc. Am. A*, Vol. 24, No. 1, 156–162, 2007.
83. Tang, H., X. Yuan, and B. Wang, "Scintillation optimization of linear Gaussian beam array propagating through weak turbulence," *J. Mod. Opt.*, Vol. 60, No. 20, 1830–1837, 2013.
84. Gu, Y. and G. Gbur, "Scintillation of Airy beam arrays in atmospheric turbulence," *Opt. Lett.*, Vol. 35, No. 20, 3456–3458, 2010.

85. Gu, Y., O. Korotkova, and G. Gbur, "Scintillation of nonuniformly polarized beams in atmospheric turbulence," *Opt. Lett.*, Vol. 34, No. 15, 2261–2263, 2009.
86. Chen, Y., Y. Cai, H. T. Eyyuboglu, and Y. Baykal, "Scintillation properties of dark hollow beams in a weak turbulent atmosphere," *Appl. Phys. B*, Vol. 90, No. 1, 87–92, 2008.
87. Cai, Y., Y. Chen, H. T. Eyyuboglu, and Y. Baykal, "Scintillation index of elliptical Gaussian beam in turbulent atmosphere," *Opt. Lett.*, Vol. 32, No. 16, 2405–2407, 2007.
88. Polynkin, P., A. Peleg, L. Klein, and T. Rhoadarmer, "Optimized multiemitter beams for free-space optical communications through turbulent atmosphere," *Opt. Lett.*, Vol. 32, No. 8, 885–887, 2007.
89. Chen, Z., C. Li, P. Ding, J. Pu, and D. Zhao, "Experimental investigation on the scintillation index of vortex beams propagating in simulated atmospheric turbulence," *Appl. Phys. B*, Vol. 107, No. 2, 469–472, 2012.
90. Baykal, Y., H. T. Eyyuboglu, and Y. Cai, "Scintillations of partially coherent multiple Gaussian beams in turbulence," *Appl. Opt.*, Vol. 48, No. 10, 1943–1954, 2009.
91. Wang, F., Y. Cai, H. T. Eyyuboglu, and Y. Baykal, "Twist phase-induced reduction in scintillation of a partially coherent beam in turbulent atmosphere," *Opt. Lett.*, Vol. 37, No. 2, 184–186, 2012.
92. Korotkova, O., L. C. Andrews, and R. L. Phillips, "Model for a partially coherent Gaussian beam in atmospheric turbulence with application in lasercom," *Opt. Eng.*, Vol. 43, No. 2, 330–341, 2004.
93. Korotkova, O., "Scintillation index of a stochastic electromagnetic beam propagating in random media," *Opt. Commun.*, Vol. 281, No. 9, 2342–2348, 2008.
94. Berman, G. P. and A. A. Chumak, "Photon distribution function for long-distance propagation of partially coherent beams through the turbulent atmosphere," *Phys. Rev. A*, Vol. 71, No. 1, 013805, 2006.
95. Wang, F., X. Liu, L. Liu, Y. Yuan, and Y. Cai, "Experimental study of the scintillation index of a radially polarized beam with controllable spatial coherence," *Appl. Phys. Lett.*, Vol. 103, No. 9, 091102, 2013.
96. Liu, X., Y. Shen, L. Liu, F. Wang, and Y. Cai, "Experimental demonstration of vortex phase-induced reduction in scintillation of a partially coherent beam," *Opt. Lett.*, Vol. 38, No. 24, 5323–5326, 2013.
97. Chen, Z., S. Cui, L. Zhang, C. Sun, M. Xiong, and J. Pu, "Measuring the intensity fluctuation of partially coherent radially polarized beams in atmospheric turbulence," *Opt. Express*, Vol. 22, No. 15, 18278–18283, 2014.
98. Avramov-Zamurovic, S., C. Nelson, R. Malek-Madani, and O. Korotkova, "Polarization-induced reduction in scintillation of optical beams propagating in simulated turbulent atmospheric channels," *Wav. Ran. Med.*, Vol. 24, No. 4, 452–462, 2014.
99. Korotkova, O., S. Avramov-Zamurovic, C. Nelson, R. Malek-Madani, Y. Gu, and G. Gbur, "Scintillation reduction in multi-Gaussian Schell-model beams propagating in atmospheric turbulence," *Proc. of SPIE*, Vol. 9224, 92240M, 2014.
100. Chernov, L. A., *Wave Propagation in a Random Medium,* Dover, New York, 1967.
101. Beckmann, P., "Signal degeneration in laser beams propagated through a turbulent atmosphere," *Radio Sci.*, Vol. 69D, No. 4, 629–640, 1965.
102. Chiba, T., "Spot dancing of the Laser beam propagated through the atmosphere," *Appl. Opt.*, Vol. 10, No. 11, 2456–2461, 1971.
103. Churnside, J. H. and R. J. Lataitis, "Wander of an optical beam in the turbulent atmosphere," *Appl. Opt.*, Vol. 29, No. 7, 928–930, 1990.
104. Klyatskin, V. I. and A. I. Kon, "On the displacement of spatially bounded light beams in a turbulent medium in the Markovian-random-process approximation," *Radio, Quan. Electron.*, Vol. 15, No. 9, 1056–1061, 1972.
105. Mironov, V. L. and V. V. Nosov, "On the theory of spatially limited light beam displacements in a randomly inhomogeneous medium," *J. Opt. Soc. Am.*, Vol. 67, No. 8, 1073–1080, 1977.

106. Andrews, L. C., R. L. Phillips, R. J. Sasiela, and R. Parenti, "Beam wander effects on the scintillation index of a focused beam," *Proc. of SPIE*, Vol. 5793, 2005.
107. Tofsted, D. H., "Outer-scale effects on beam-wander and angle-of-arrival variances," *Appl. Opt.*, Vol. 31, No. 27, 5865–5870, 1992.
108. Eyyuboglu, H. T. and C. Z. Cil, "Beam wander of dark hollow, flat-topped and annular beams," *Appl. Phys. B*, Vol. 93, Nos. 2–3, 595–604, 2008.
109. Cil, C. Z., H. T. Eyyuboglu, Y. Baykal, and Y. Cai, "Beam wander characteristics of cos and cosh-Gaussian beams," *Appl. Phys. B*, Vol. 95, No.4, 763–771, 2009.
110. Cil, C. Z., H. T. Eyyuboglu, Y. Baykal, O. Korotkova, and Y. Cai, "Beam wander of J_0- and I_0-Bessel Gaussian beams propagating in turbulent atmosphere," *Appl. Phys. B*, Vol. 98, No. 1, 195–202, 2010.
111. Aksenov, V. P., V. V. Kolosov, and C. E. Pogutsa, "The influence of the vortex phase on the random wandering of a Laguerre-Gaussian beam propagating in a turbulent atmosphere: A numerical experiment," *J. Opt.*, Vol. 15, No. 4, 044007, 2013.
112. Aksenov, V. P., V. V. Kolosov, and C. E. Pogutsa, "Random wandering of laser beams with orbital angular momentum during propagation through atmospheric turbulence," *Appl. Opt.*, Vol. 53, No. 17, 3607–3614, 2014.
113. Wen, W. and X. Chu, "Beam wander of an Airy beam with a spiral phase," *J. Opt. Soc. Am. A*, Vol. 31, No. 4, 685–690, 2014.
114. Funes, G., D. Gulich, L. Zunino, D. G. Perez, and M. Garavaglia, "Behavior of the laser beam wandering variance with the turbulent path length," *Opt. Commun.*, Vol. 272, No. 2, 476–479, 2007.
115. Kaushal, H., V. Kumar, A. Dutta, H. Aennam, V. Jain, S. Kar, and J. Joseph, "Experimental study on beam wander under varying atmospheric turbulence conditions," *IEEE Photo. Tech. Lett.*, Vol. 23, No. 22, 1691–1693, 2011.
116. Berman, G. P., A. A. Chumak, and V. N. Gorshkov, "Beam wandering in the atmosphere: The effect of partial coherence," *Phys. Rev. E*, Vol. 76, No. 5, 056606, 2007.
117. Xiao, X. and D. G. Voelz, "Beam wander analysis for focused partially coherent beams propagating in turbulence," *Opt. Eng.*, Vol. 51, No. 2, 026001, 2012.
118. Song, Y., Z. Chen, T. Wang, G. Wu, H. Guo, and W. Gu, "Beam wander of electromagnetic Gaussian-Schell model beams propagating in atmospheric turbulence," *Appl. Opt.*, Vol. 51, No. 31, 7581–7585, 2012.
119. Liu, X., F. Wang, C. Wei, and Y. Cai, "Experimental study of turbulence-induced beam wander and deformation of a partially coherent beam," *Opt. Lett.*, Vol. 39, No. 11, 3336–3339, 2013.
120. Korotkova, O., L. C. Andrews, and R. L. Phillips, "LIDAR model for a rough-surface target: Method of partial coherence," *Proc. SPIE*, Vol. 5237, 49–60, 2003.
121. Korotkova, O., L. C. Andrews, and R. L. Phillips, "Laser radar in turbulent atmosphere: Effect of Target with arbitrary roughness on II and IV order statistics of Gaussian beam," *Proc. SPIE*, Vol. 5086, 173–183, 2003.
122. Korotkova, O., Y. Cai, and E. Watson, "Stochastic electromagnetic beams for LIDAR systems operating through turbulent atmosphere," *Appl. Phys. B*, Vol. 94, No. 4, 681–690, 2009.
123. Sahin, S., Z. Tong, and O. Korotkova, "Sensing of semi-rough targets embedded in atmospheric turbulence by means of stochastic electromagnetic beams," *Opt. Commun.*, Vol. 283, No. 22, 4512–4518, 2010.
124. Wu, G. and Y. Cai, "Detection of a semi-rough target in turbulent atmosphere by a partially coherent beam," *Opt. Lett.*, Vol. 36, No. 10, 1939–1942, 2011.
125. Wang, F. and Y. Cai, "Experimental observation of fractional Fourier transform for a partially coherent optical beam with Gaussian statistics," *J. Opt. Soc. Am. A*, Vol. 24, No. 7, 1937–1944, 2007.
126. Wang, F. and Y. Cai, "Experimental generation of a partially coherent flat-topped beam," *Opt. Lett.*, Vol. 33, No. 16, 1795–1797, 2008.

127. Zhao, C., Y. Cai, F. Wang, X. Lu, and Y. Wang, "Generation of a high-quality partially coherent dark hollow beam with a multimode fiber," *Opt. Lett.*, Vol. 33, No. 12, 1389–1391, 2008.
128. Wang, F., G. Wu, X. Liu, S. Zhu, and Y. Cai, "Experimental measurement of the beam parameters of an electromagnetic Gaussian Schell-model source," *Opt. Lett.*, Vol. 36, No. 14, 2722–2724, 2011.
129. Wang, F., S. Zhu, and Y. Cai, "Experimental study of the focusing properties of a Gaussian Schell-model vortex beam," *Opt. Lett.*, Vol. 36, No. 16, 3281–3283, 2011.
130. Wang, F., Y. Cai, Y. Dong, and O. Korotkova, "Experimental generation of a radially polarized beam with controllable spatial coherence," *Appl. Phys. Lett.*, Vol. 100, No. 5, 051108, 2012.
131. Zhao, C., F. Wang, Y. Dong, Y. Han, and Y. Cai, "Effect of spatial coherence on determining the topological charge of a vortex beam," *Appl. Phys. Lett.*, Vol. 101, No. 26, 261104, 2012.
132. Wang, F., X. Liu, Y. Yuan, and Y. Cai, "Experimental generation of partially coherent beams with different complex degrees of coherence," *Opt. Lett.*, Vol. 38, No. 11, 1814–1816, 2013.
133. Chen, Y. and Y. Cai, "Generation of a controllable optical cage by focusing a Laguerre-Gaussian correlated Schell-model beam," *Opt. Lett.*, Vol. 39, No. 9, 2549–2552, 2014.
134. Chen, Y., F. Wang, C. Zhao, and Y. Cai, "Experimental demonstration of a Laguerre-Gaussian correlated Schell-model vortex beam," *Opt. Express*, Vol. 22, No. 5, 5826–5838, 2014.
135. Chen, Y., F. Wang, L. Liu, C. Zhao, Y. Cai, and O. Korotkova, "Generation and propagation of a partially coherent vector beam with special correlation functions," *Phys. Rev. A*, Vol. 89, No. 1, 013801, 2014.
136. Liang, C., F. Wang, X. Liu, Y. Cai, and O. Korotkova, "Experimental generation of cosine-Gaussian-correlated Schell-model beams with rectangular symmetry," *Opt. Lett.*, Vol. 39, No. 4, 769–772, 2014.
137. Wang, F., C. Liang, Y. Yuan, and Y. Cai, "Generalized multi-Gaussian correlated Schell-model beam: From theory to experiment," *Opt. Express*, Vol. 22, No. 19, 23456–23464, 2014.
138. Chen, Y., J. Gu, F. Wang, and Y. Cai, "Self-splitting properties of a Hermite-Gaussian correlated Schell-model beam," *Phys. Rev. A*, Vol. 91, No. 1, 013823, 2015.
139. Chen, Y., L. Liu, F. Wang, C. Zhao, and Y. Cai, "Elliptical Laguerre-Gaussian correlated Schell-model beam," *Opt. Express*, Vol. 22, No. 11, 13975–13987, 2014.
140. Cai, Y., Y. Chen, and F. Wang, "Generation and propagation of partially coherent beams with non-conventional correlation functions: A review," *J. Opt. Soc. Am. A*, Vol. 31, No. 9, 2083–2096, 2014.
141. Gbur, G., "Partially coherent beam propagation in atmospheric turbulence," *J. Opt. Soc. Am. A*, Vol. 31, No. 9, 2038–2045, 2014.